Bulletin of the Earthquake
Research Institute
Vol. 53 (1978), pp. 49-130

2. A *Transportable Apparatus for Absolute Measurement of Gravity.*

By Ichiro Murata,

Earthquake Research Institute.

(Received January 5, 1978.)

Abstract

A transportable apparatus for an absolute measurement of gravity has been constructed for the purpose of detecting secular variations of gravity. First of all, the significance of the absolute measurement of gravity is outlined in this paper.

The principle of measurement adopted here is the simple free fall, on the basis of the well-known relation between falling distance, falling time and acceleration of gravity. Using a cat's eye as a falling object, a Michelson interferometer measures the falling distance comparatively with the wavelength of a He-Ne laser light. Interference fringes for 30 cm falling distance are continuously recorded on a recording film with 1 ms sampling intervals which are accurately controlled by a frequency standard. Phase angles of interference fringes at every 1 ms interval are taken into consideration but direct counting of the number of interference fringes is unnecessary in the present apparatus. The method of data processing, in which the falling distance is counted from time to time on phase angle data, is one of the distinct features of the present apparatus, and proves to be very effective in both detecting details of falling motion and simplifying the apparatus. Furthermore, we describe disturbing factors such as the inaccuracy in wavelength of laser light, the vertical gradient of gravity, residual gas and imcompleteness of the optical character of a falling object.

Secondly, the result of experimental observations at the Matsushiro Seismological Observatory is reported. The gravity value obtained from twenty-one test drops is as follows:

$$g_{OBS} = 979\ 770.131 \pm 0.010 \text{ mGal.}$$

This is very close to the corresponding value derived from that of the Matsushiro First-order Gravity Station of the Geographical Survey Institute;

$$g_{DRV} = 979\ 770.19 \pm 0.1 \text{ mGal.}$$

The main sources of standard error of a single drop of 0.038 mGal have been estimated as the inaccurate setting of the wavelength of

laser light and microtremors. Inaccuracy in wavelength causes a 0.020 mGal error, but it will be overcome by introducing an iodine saturated absorption stabilized He-Ne laser with an accuracy in wavelength of 1×10^{-9}. Microtremor effect on gravity amounts to about 0.026 mGal, but can be minimized by monitoring ground vibrations with a seismometer. It is concluded that the high efficiency and the practicability of the present apparatus have been confirmed through the experiment and the data analyses.

Contents

1. Introduction

Gravity measuring method is usually divided into two categories, that is, absolute measurement and relative measurement. Although such a classification of measurements is available not only for gravity measurement but for other fields of sciences, it has a special significance in gravity measurement in comparison with the other fields.

The advantage of relative measurement in gravity lies in the fact that the gravity value at a station is relatively determined to that at the base station, where the gravity value has been known. In the case of a relative pendulum measurement, the apparatus is swung at these two stations and the gravity value is obtained from the swinging periods of the pendulum at both stations on the basis of the familiar relation between gravity and period of a pendulum. As for the case of a spring-balance type gravity meter, the linear relation between gravity difference and the variation in the strain of a spring in a gravity meter is utilized for relative measurements. Both methods are essentially the same from the viewpoint that measurements of gravity are carried out comparatively with the results obtained at the base station.

In contrast with relative measurement, absolute measurement in gravity is based on the method that gravity value at a site is determined independently of gravity value at any other stations.

Comparing these two kinds of methods from a point of view of facility, the relative measurement has a great advantage over the absolute measurement. This implies the fact that many unknown disturbing factors common to all station gravimetries can be eliminated in a relative measurement by taking the difference between observed values. On the other hand, an absolute gravity measurement is relatively difficult to be

independently determined from station to station. Despite such a difficulty, it is considered to be very important to determine an absolute gravity from following geodetic and geophysical necessities.

First, the gravity observation network cannot be well established by relative measurements alone. The base-station control should be made by absolute measurements at one or several stations in the network.

Second, the unification of the global gravity network can be realized by the absolute gravimetry. In relative measurement it is inevitable to have to transport a measuring instrument between observing stations. Transportation sometimes works as a serious cause of error, such as irregular drift or tare in spring-balance type gravity meter observations, despite the vibrations-proof device for keeping the good measuring condition of the instrument. If a change in the instrumental condition exceeds a tolerable limit, it may possibly cause errors in the obtained result. These kinds of error occur from complicated disturbances, such as an ambient temperature change and mechanical vibrations during transportation, so that, although the amount of errors are usually accumulated in proportion to transportation distance and time duration, it is almost impossible to compensate accurately. Therefore, the gravity values obtained in relative measurements include some ambiguities, which have been investigated by comparing simultaneous observations by means of several LaCoste-Romberg gravity meters (MURATA, 1970). The test concluded that the accuracy of 0.02 mGal of gravity measurements is hardly attainable even after careful operations, although attention should be paid to the fact that such an accuracy indicates discrepancies amongst the results of the gravity meters used in the test survey and it does not necessarily give a definite conclusion about the difference between the true value and the observed one. It can also be considered that this result shows a limit to the accuracy of the relative gravity measurement, although exceptional cases have been reported (HONKASALO, 1970; LAMBERT et al., 1977). In the case of long-distance and long-term observations such as an international gravimetric connection, decrease in accuracy is inevitable. The International Gravity Standardization Net 1971 has reported that "The system provides gravity values with standard errors less than 0.1 mGal over the gravity range of the earth." (I.G.S.N. 71, Special Publication No. 4, International Association of Geodesy).

Transportation of the absolute gravity meter is also necessary in field work for base-station control or gravimetric connection in which several stations should be controlled by the same instrument. In this case, however, errors due to transportation do not exist essentially in absolute measurement, because the gravity values are independently determined from those at the other stations.

Another interest in absolute measurement comes from a viewpoint of geophysics with an application to the detection of secular variations in gravity. Secular changes in gravity, if any, may be separated into two classes; rather short-period changes related to the crustal tectonic phenomena such as earthquakes and the related land-deformations, longer-period ones related to the earth's global phenomena such as continental drift or core-mantle coupling. Several studies both theoretical and observational have been made about this kind of problem and the probabilities of detecting a secular change in gravity have been discussed (BARNES, 1966; BARTA, 1971; BOULANGER et al., 1973).

TAJIMA (1975) has brought forward considerable evidence of the existence of variations in gravity, especially on the basis of the observational facts taken during the Matsushiro earthquake swarms. But, almost all the investigations on the time variation in gravity which have been studied so far, have treated the data relatively determined in a limited area. If a gravity change exists in a large area, the base-station control and the accurate estimation on the gravity time-variation may be difficult. In extreme cases such as world-wide gravity changes covering the entire earth, relative measurement is quite incompetent to detect them. In order to overcome such measuring difficulties, an absolute gravimetry plays an important role in determination of global time-variation in gravity.

Furthermore, the necessity of absolute measurement concerns metrology. Gravity is one of the most stable forces among many kinds of forces which are available in metrological laboratories as a standard force. It is needless to say that the absolute value of gravity must be known for this purpose, for example, it is necessary to determine the specified value of pressure to realize the defined fixed point of temperature in the international practical temperature scale. The pressure, hence the gravity value, must be known with an accuracy of 3×10^{-6} to determine the boiling point of water under the pressure of 1 atm within an accuracy of 1×10^{-4}°C. The absolute measurement of an electric current, the definition of an Ampere which is one of the fundamental units in International System of Units, is carried out by means of a current balance in which the attraction between electric currents is counterbalanced with the gravitational force.

A situation of the absolute measurement of gravity in geodesy can be also considered from the viewpoint of astronomical geodesy. Latitude variations caused by polar motion result in gravity changes. For example, if latitude variation in the middle latitude zone is 0.4″, it causes about 9μGal change in gravity. This fact suggests a possibility of detecting polar motion by a non-astronomical method. But the gravity change by

polar motion has global distribution, hence without absolute measurement its detection is impossible. Usual astro-geodetic observations, including latitude observations are carried out on the basis of local vertical at the observation site. This means that local transformation of the equipotential surface of the earth's gravitational field, whatever its cause may be, brings about an apparent change in observational results. The monitoring of equipotential surface transformation is, therefore, essential and the gravity observation by the absolute method can play this role. These may be the reasons for the introduction of Sakuma's apparatus (it will be explained later) into the International Latitude Observatory of Mizusawa.

Attention should be paid to the present state of arts in physics, in which instruments appear that utilize transitions between energy levels of atoms such as an atomic clock and a laser. This means that the absolute measurement of gravity is able to be carried out without using conventional standards such as a crystal clock and an end standard, and that it will be free from the instrumental drift which has inevitably accompanied it so far. It can be said that the combination of quantum phenomena with absolute gravity measurement produces the possibility of using absolute measurement as a reliable method to detect secular changes in gravity for the first time.

The construction of an apparatus for absolute measurement was planned, taking the circumstances described above into consideration in the present work. The technical background today makes it possible to produce such an apparatus which has an measuring accuracy of 0.01 mGal or better. There exist already the famous instruments for absolute measurement, that is Sakuma's and Faller's. But the author's intention was to build a new instrument which has a small size and a high portability, stability and accuracy level. That instrument has to be fitted for field work since it will be used in the geophysically interesting regions. Field observation is essential especially in Japan where the realization of earthquake prediction is urged. This work started with such an ambitious plan.

The following is the sketch of the constitution of this paper. An outline of the method of absolute measurements carried out before the present work is reviewed in Chapter 2. This chapter will work as a comparison between the present apparatus and others. Chapters 3, 4 and 5 are the explanation of the structure and operation of the present instrument. Chapter 6 on data processing is devoted to explaining how to obtain a result from the observed data. The method of data processing adopted to the present instrument is unique and very effective. In Chapter 7, we discuss several disturbing factors which might affect the

result. There are, of course, many other disturbing factors which have to be taken into account in some cases, such as light pressure and Eötvös effect. But these are neglected here since the effects are considered to be too small for present instrument. The results of test observations which have confirmed the high efficiency of the instrument and some other interesting phenomena revealed at the same time will be treated in the remaining chapters.

2. An Outline of Absolute Measurements of Gravity

2.1. Reversible Pendulum Method

Gravity was determined by absolute measurements, in a sense, in the early stage of its history. The name of J. Borda is still familiar through his physical pendulum used for determining the precise length of a pendulum of a one second period on a 45°N latitude and defining a length standard. Absolute gravity measurement in a modern sense, however' began later at the time of H. Kater who introduced the classification of gravity measurement into relative and absolute measurements. He made many observations of gravity differences by means of pendulums and moreover devised a reversible pendulum for absolute measurements. The effect of the surrounding air on the motion of a pendulum can be separated into buoyancy and inertial resistance as presented by BESSEL (1850), STOKES (1901) and others. J. G. Repsold designed the pendulum which could eliminate the effect of inertial air resistance. The pendulum of this type is historically famous for the experiment conducted by KÜHNEN and FURTWÄNGLER (1909), which was made at the Geodetic Institute in Potsdam under the direction of Helmert. It is said that there had been no observations exceeding the accuracy of their test until the beginning of 1930's, so that the result of this experiment has been adopted as the fundamental value of the current Potsdam gravity system.

There are two kinds of measuring systems, reversible pendulum method and free fall method. The reversible pendulum method was a method only available before 1945. It is well-known that, in the reversible pendulum, the distance between the axes of rotations in normal and reversal positions is equivalent to the length of an idealized simple pendulum having the same period, provided that the periods in both positions are equal. This is the principle of the reversible pendulum method. It may be worth while pointing out that the gravity value by which the motion of the pendulum is regulated corresponds to the value not at the center of gravity of the pendulum but at the position of the lower axis of rotation. As for the work of KÜHNEN and FURTWÄNGLER (1909), they used five pendulums, four having one second periods and the fifth having 0.5

second period. These pendulums were so designed that they had symmetrical shapes with respect to a horizontal plane in order to cancel the inertial effect of accompanying air.

The experiments were carried out under atmospheric air pressure by attaching knife edges to the pendulum at the first stage of the work. The same pair of knife edges were used for each pendulum in succession in order to eliminate the effect of the curvature of knife edge, the accurate measurement of which is very difficult even now. The surrounding air pressure was reduced later and the arrangement of the knife edge and bearing plane was inverted, that is the bearing planes were attached to the pendulum and the knife edge was fixed to the support. Such an arrangement of the knife edge and bearing plane has been widely adopted in other observations since then because of its advantage of measuring the separation between the two axes of rotation. The periods were reduced to a perfect vacuum by using the empirical relation between the period and the air density.

It has been known that Kühnen and Furtwängler's result at Potsdam was too large by about 14 mGal. This excess is mainly due to the extraporation of the result to the zero mass pendulum. The re-evaluations of the result have been reported by several authors (DRYDEN, 1942; JEFFREYS, 1949).

After the work of Kühnen and Furtwängler several reversible pendulum observations were successively carried out. Among them; HEYL and COOK's (1936) measurement at the National Bureau of Standards, Washington and CLARK's (1939) at the National Physical Laboratory, Teddington were historically famous. These two works were originally intended for a metrological purpose of realizing a standard of force. The pendulum which was used by Heyl and Cook was in the shape of a cylindrical pipe, made of fused silica, about 160 cm in length and 100 cm in reduced length. The bearing plane was attached to the pendulum and the knife edge was rigidly fixed to the wall and composed the rotation axis. Ambient air pressure was reduced to 10 Pa (0.1 mbar), and its effect on the observed gravity value reached to 0.6 mGal because of the small density of fused silica. The effect of the bending of the oscillating pendulum was rather large (several mGal) because the pendulum did not have rigid style. This pendulum was used again at the University of Buenos Aires by E. Bagliett.

CLARK (1939) used a Y-alloy pendulum. Special attention was paid to the bending of the pendulum and it was formed in the shape of I-beam. The beam of pendulum was 100 cm long. The upper and lower ends of the beam were lapped into the parallel planes and the distance between both the ends was measured by interferometry. Since the two rectangular

blocks of Delta-metal which worked as bearing planes were firmly bolted to the end planes of the pendulum, the distance between both the ends was equivalent to the reduced length of pendulum. An additional mass block was further attached to one end to coincide in the period in both normal and reversal positions. A knife edge was fixed to the firm base support. The sway of the support was estimated from the induced oscillation of the second pendulum which was set on the same support. As Y-alloy is paramagnetic, geomagnetism did not affect the motion of pendulum. Since its thermal expansion coefficient is not so small that the effect of temperature was serious, the controlled heater was installed around the apparatus and the platinum resistance thermometers were set at three points along the pendulum. Room temperature was controlled to 20°C. Inside pressure was reduced to 0.7 Pa and the effect of surrounding air was negligible. In contrast with the optical systems adopted by Kühnen and Furtwängler and Heyl and Cook, Clark's system for timing the motion of the pendulum was to obtain electrical signals with mechanical contact between the needle point at the tip of the pendulum and the surface of mercury pool which was set at the bottom of the instrument.

There were several other pendulum observations to be noticed. The works of AGALETSKY, YEGOROV and MARTSINYAK (1959) and SCHÜLER, HARNISCH, FISCHER and FREY (1971) can be quoted as modern type of measurements. In spite of the long history of pendulum observations in absolute measurement since Kühnen and Furtwängler, its observational accuracy has not shown remarkable progress. It is mainly due to the effect of the contact between a knife edge and a bearing plane on the motion of pendulum which is very hard to analyse. It is also the author's experience in relative measurement by means of a pendulum. The adoption of the free fall method is a natural conclusion in designing the present apparatus. But it is worth while to point out that the pendulum observation has a merit which cannot be realized in the free fall method. It is that the measuring time can be prolonged and it is advantageous to eliminate the effect of ground vibrations.

2.2. Free Fall Method

The timing technique has been developed since the 1940's especially with close concern to the radar. The possibility of applying this technique to the measurement of the acceleration of a falling body in the gravity field has been recognized. The proposal of this kind was first made by GULLIET (1938). VOLET (1946) pointed out that the measurement of gravity is possible by taking a high speed photograph of a falling graduated scale. He also proposed the symmetrical free fall method, in

which the falling object is thrown vertically up and timings of the object passing through the reference plane are taken at both upward and downward passages. This method made it possible to increase the accuracy of measurement.

The free fall method in absolute gravity measurement is classified into two types. One is a symmetrical free fall method and the other is a simple free fall in a narrow sense. There have been several measurements by means of the free fall method up to the present. THULIN (1961), PRESTON-THOMAS (1960), FALLER (1963), TATE (1966), COOK (1967), SAKUMA (1971), BELL (1973) and SENDA (1971) have all carried out measurements for the purpose of metrology and their apparatuses were so large that the transportations were difficult except for Faller's instrument. We will briefly introduce here Faller's and Sakuma's instruments as typical examples of simple and symmetrical free fall methods respectively.

2.2.1. Faller's Instrument

J. Faller measured the falling distance by a He-Ne stabilized laser utilizing its wavelength as scale graduations. The optical system for measuring the falling distance is equivalent to that of a Michelson interferometer, in which one of a cubic corner type reflecting mirror works as a falling object. Falling distance is about 1 m and it is measured with an accuracy of 1×10^{-8}, with timing done by a crystal clock with an accuracy of 1×10^{-9}. A long period vertical seismometer is mounted on top of the falling chamber to monitor external vibrations. The reference mirror of the interferometer is mounted on the weight of the seismometer, in which the reference point of the optical distance measurement is inertially fixed.

The measurement of the falling distance is carried out by two sets of counters, counting the number of interference fringes as the falling object moves. These counters start the counting of fringes simultaneously about 0.013 s after the beginning of free fall. One counter stops after a fixed time interval (about 0.18 s) which is controlled by a crystal clock. The second counter continues counting for a period of about 0.36 s. Thus two sets of measured time and distance are obtained for each drop. If we measure (t_1, m_1) and (t_2, m_2), where t_i and m_i are the falling time and distance (in the fringe count) respectively, the gravity value g is calculated according to the following relation:

$$g=\frac{\lambda\{m_2-m_1(t_2/t_1)\}}{t_2^2-t_1t_2} \tag{2-1}$$

in which λ is the wavelength of laser light used. The vertical gradient of gravity is supposed be zero here.

The transportability and the direct measurement of the falling distance at the time of the fall by using a laser beam are distinctive features of this instrument. (FALLER, 1965a, b, 1967; HAMMOND et al., 1971)

2.2.2. Sakuma's Instrument

A. Sakuma's instrument is believed to have the highest accuracy in the world at present. The simple free fall system is necessary to provide at least two fixed parts of lengths for measuring falling distance, whereas in contrast, only one falling distance is of use for the symmetrical free fall system. The two horizontal planes, the separation of which is equal to this falling distance, work as timing positions. The transit of the falling object across these planes produces timing signals as it passes through each plane twice; upward and downward. If we denote the time intervals between two passages at the upper and lower planes by t_2 and t_1 respectively and the distance between two planes by h, then the gravity value is given by

$$g=\frac{8h}{t_1^2-t_2^2}. \tag{2-2}$$

In general, timing error in such a symmetrical free fall method can be kept to a minimum because the speeds of the falling object are equal at the same elevation, consequently the time delays occurring in the electronic circuit are equal. Moreover, the symmetrical free fall system has a great advantage over the simple free fall system, in that, the great part of the effect due to the resistance of existing gas can be canceled out, because the direction of the resistance force becomes reversed at the passage of the apex of trajectory of motion.

Although the symmetrical free fall method has many advantages over the simple free fall method, it is considerably difficult to keep the attitude of a falling object constant during its motion, in other words, the soft launching of the falling object, is very hard to attain. Fortunately, the advancement in electronics and the vacuum technique covers the corresponding disadvantages of the simple free fall method, and consequently, it is not necessary to adopt the symmetrical free fall method, now, in designing a transportable instrument.

In Sakuma's instrument, the reflecting mirror, which is the falling object, is also of a cubic corner type, and the detection of the transit of the falling object is made by a Michelson interferometer. Without counting the numbers of interference fringes, unlike Faller's instrument, Sakuma utilizes the white light interference which occurs only when both separations of the two reflecting mirrors from the beam splitter become

equal. The interferometer has two fixed reference mirrors in the near and far positions which correspond to the upper and lower planes of transition respectively. These two reference mirrors themselves form an end standard. Its length is calibrated by optical interferometry using Kr light, the wavelength of which is the current standard of length. The white light fringe patterns and time signals from the crystal clock are simultaneously displayed on the oscilloscope and are photographed (SAKUMA, 1963, 71, 73).

3. Measuring System

Our purpose of constructing an absolute measurement apparatus of gravity is to detect secular change in gravity in geophysically interesting regions. It is desirable to design an instrument as simple as possible and to make it transportable. Taking these requirements into account, the simple free fall method was adopted for the present design.

The principle of measurement by the simple free fall method is as follows. The relation between the falling time (t) and the falling distance (s) of a falling body in the uniform gravity field is

$$s=\frac{1}{2}gt^2+v_0t+s_0 \tag{3-1}$$

where, g, v_0 and s_0 are acceleration of gravity, initial velocity and initial position, respectively. In other words, absolute gravity measurement by the simple free fall method results in measurement of falling distance with falling time. The observation in the simple free fall method can be usually classified into the distance preset method and the time preset method. In the distance preset method, the observation is carried out by measuring the travelling time of the object falling through several horizontal planes, the separations of which have been accurately determined in advance. In the time preset method, to the contrary, the falling distance is measured, which corresponds to the precisely predetermined time duration. It is impossible to drop (or to throw up) the falling object with such precisely controlled initial velocity that its effect on the result can be checked off with a sufficient accuracy. Therefore, at least two predetermined distances (or time intervals) are required in an actual measurement. In the present study the time preset method has been adopted. The falling distance is measured by an optical interference of laser light and it is determined directly at the time of the fall with the wavelength of the laser light as a scale graduation.

It is one of the distinctive features of the present instrument that the number of timing positions is large, because its sampling interval is

1 ms, in contrast with other instruments which have only two or three reference points. The falling distance in this instrument is about 30 cm and the corresponding falling time is about 0.25 s. Therefore 250 recordings on the falling distance are obtained for a single drop. The multiple measurement of falling distance makes it possible to observe the motion of the falling object in detail and increase the accuracy of measurement effectively.

4. Apparatus

As shown in Figs. 4-1 and 4-2, our instrument is divided into the main part and the recording part. The main part is separated into the vacuum chamber, the evacuation system, the falling object and the optical system to measure the falling distance of the object. The recording part is composed of the oscilloscope, the recording camera, the electronic circuit and the time standard. The details of each part will be described below.

4.1. Vacuum Chamber

The main part of the chamber is made of a stainless steel pipe 11 cm in inner diameter. It contains the handling mechanism for falling object.

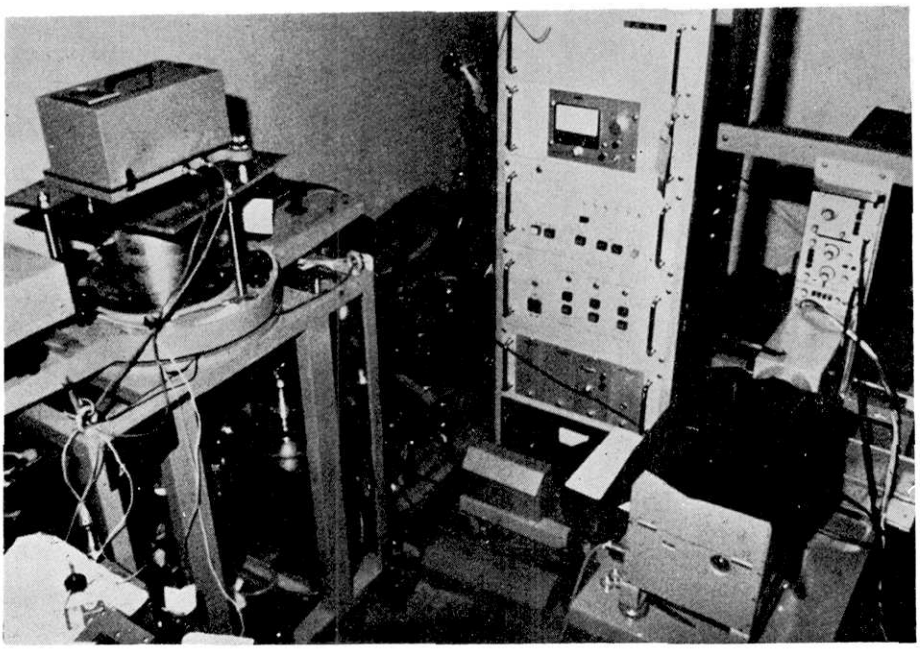

Fig. 4-1. Absolute gravity measurement apparatus.
left: Main part (vacuum chamber and optical system)
right: Power supply and recording system

The upper part of the chamber is widened to 20.8 cm in diameter, containing the optical system to measure the falling distance. A window having a glass lid opens at the side wall for setting a falling object into the chamber. Rotations of two shafts protruding at the bottom of the chamber make it possible to operate the inside mechanism to catch and set the falling object. The vacuum chamber also has two arm pipes each of which is connected to a diffusion pump and an ion pump respectively. This vacuum chamber is separated into three parts: the falling chamber, the top chamber and the supporting frame with the evacuation pumps. This separation makes it easy to transport the whole apparatus.

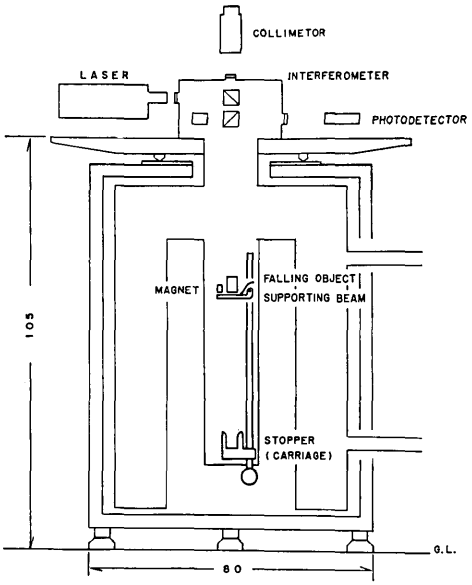

Fig. 4-2. Schematic construction of the main part.

4.2. Evacuation System

Coarse evacuation is carried out by the oil diffusion pump until the inside pressure reaches 10^{-5} Torr. Then evacuation is continued by the ion pump. The ion sputter pump has no mechanically moving part, so that it hardly disturbs the gravity measurement with mechanical vibrations and accordingly makes it unnecessary to interrupt the evacuation during the fall time. This means that the transient state of vacuum which happens at the time of the evacuation stop in the use of a mechanical pump can be avoided. The degree of vacuum is monitored by a Geissler tube in the beginning of evacuation and is measured by means of an ionization vacuum gauge.

4.3. Handling Device

Inside the vacuum chamber, a handling device catches, supports and resets the falling object by rotating handles at the bottom of the vacuum chamber. The structure of this device is shown in Fig. 4-3. The right side handle moves the carriage up and down, which rests at the bottom of the chamber and works as the stopper of the falling object at its fall. Near the top of the vacuum chamber, catching hooks hold the falling object, a supporting beam sets it at the starting position and an electric

magnet retains the supporting beam horizontally. The supporting beam is geared to the carriage. The catching hooks work by turning the left side handle at the bottom of the chamber. The bottom of the carriage is supported by a spring, sliding relative to the Teflon-made side wall. It works as a buffer against a shock on the fall. The supporting beam has three gold bosses of 1.5 mm high on its upper surface along the circumference of a 15 mm diameter. The setting of the supporting beam to the horizontal position thrusts up the falling object to release it from the catching hooks. The use of gold for the contact tips avoids contamination which would cause undesirable surface adhesion between the beam and the falling object.

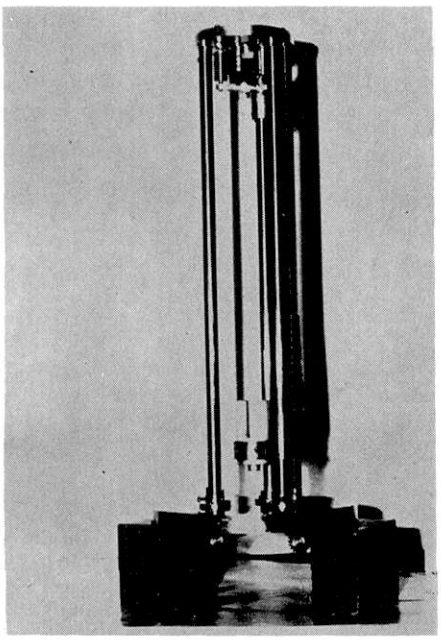

Fig. 4-3. Handling device for a falling object.

The motion of the falling object is triggered by cutting off the exciting current to the magnet which holds the supporting beam. The supporting beam releases the falling object by rotating around the horizontal pivot. There is initially some stress applied downward by a weak spring to avoid collision against the falling object.

4.4. Optical System

A Michelson-type interferometer measures the falling distance. The falling object works as one of the reflectors in the optical arms of the interferometer. The light source of interferometer is a Lamb dip stabilized He-Ne laser (LAMB, 1964). The accuracy of a laser wavelength of this type is in the order of 1×10^{-8}. If we desire to measure gravity with an accuracy of 0.01 mGal, the relative limit of the measuring errors of the falling distance must be smaller than 10^{-8}. A Lamb dip stabilized He-Ne laser meets this requirement of the stability of wavelength. It seems, however, that there remains some question on the long term stability of the wavelength (ENGELHARD, 1966), and on the pressure dependence (ENGELHARD et al., 1971). But the appearance of an iodine saturated absorption stabilized He-Ne laser overcomes this question though it cannot yet be used in the present work. An ordinary Lamb dip stabi-

lized He-Ne laser has a servo loop in its control circuit to detect a Lamb dip position and to lock the operating state there. Lamb dip position is detected by vibrating its optical resonator mirrors and monitoring the output intensity of light. The laser used in this work had adopted 500 Hz. The wavelength of the laser light fluctuates with the vibration frequency of resonator because the distance of mirrors regulates wavelength, therefore it cannot be used in its original style for this work. Taking this oscillation in wavelength into account, the servo loop is left open and a manual setting on the wavelength to the center of Lamb dip has been adopted. The optical resonator mirrors whose distance is thus adjusted are left as they are for several seconds until the falling object drops. The change in wavelength during this short time interval (several seconds) is very small and is believed not to affect the result.

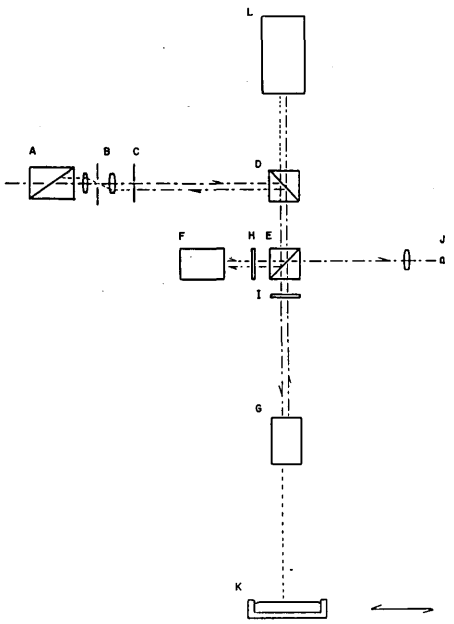

Fig. 4-4. Optical system.
A: Glan-Thompson prism, B: Beam expander, C: Diaphragm, D: Reflecting prism, E: Beam splitter, F: Fixed mirror (cat's eye), G: Falling mirror (cat's eye), H, I: quarter-wave plates, J: Photodetector, K: Mercury pool

The light from the laser first passes through a Glan-Thompson prism (denoted as A in Fig. 4-4. This note is applicable in the following.) which works as a back talk preventer (it will be explained later). Then the beam is enlarged to 2 mm in diameter by a beam expander (B), entering horizontally into the vacuum chamber. There is a right-angle prism (D) at the top, inside the vacuum chamber, to deviate the light beam vertically downward. This prism is rotated around two axes to adjust the direction of the light beam to the true vertical. The incident light is divided into two beams by a beam splitter (E) situated beneath this prism. One of the beams proceeds horizontally toward a fixed reflector (F). The other beam goes straight downward to the falling object (G). A pair of identical cat's eyes is used as the fixed reflector and the falling object. It is advisable to use the same-type reflectors taking the inversion of the image on reflection and optical aberrations into account.

It is well-known that the two return light beams reflected from

each cat's eye are combined together to form an optical interference at the beam splitter. The interference fringe causes cyclic variations in intensity with regard to the change in the difference between two optical path lengths at every half wavelength. Therefore the measurement of the falling distance of the reflectors is made by counting the number of the variations in the intensity of interference. The instantaneous amplitudes of the respective returning light beams at the beam splitter are $A \sin 2\pi(ft-2x'/\lambda)$ and $B \sin 2\pi(ft-2x/\lambda)+\phi$ for the light from the fixed reflector and the light from the falling reflector, respectively, where A and B are amplitudes of each light, f, the frequency of light (4.7×10^{14} Hz), t, the falling time, λ, the wavelength of light (633 nm), x' and x, the distance from the beam splitter to the fixed reflector, and that to the falling reflector and ϕ, representative of the phase shift on the reflection at the beam splitter. The interference intensity I after the recombination of the two light beams is written as:

$$I=R^2 \sin^2 (2\pi ft-\theta), \tag{4-1}$$

where,

$$R^2=A^2+B^2+2AB \cos\left\{2\pi\frac{2(x'-x)}{\lambda}+\phi\right\}, \tag{4-2}$$

$$\tan\theta=-\frac{A \sin (2\pi(2x'/\lambda))+B \sin (2\pi(2x/\lambda)-\phi)}{A \cos (2\pi(2x'/\lambda))+B \cos (2\pi(2x/\lambda)-\phi)}. \tag{4-3}$$

Although both phase angle and amplitude are related to x, the variation in the phase angle is far faster than that in the amplitude, hence it is enough to consider the variation in R only as the variation in intensity of interference by the change of falling distance. One cycle change in intensity corresponds to a distance variation of $\lambda/2$. This is a well-known principle of distance measurement by interferometry.

A serious problem, so called back talk, arose in association with the combination of a Michelson interferometer and a laser. This is a problem concerned with the characteristics of the laser and the reflected laser beam from the interferometer which gets back into the laser. This returning light disturbs the delicate oscillation mode of the laser, so that its optical characteristics such as wavelength, phase and output intensity fluctuate at random. To overcome such a difficulty the following countermeans are taken for the present instrument. The incident light upon the reflector is shifted from its optical axis by 2 mm. As the reflected light radiates from the symmetrical point with respect to the optical axis of the reflector, the distance between the incident and reflected rays becomes 4 mm. Hence the greater part of reflected light is cut out by a diaphragm (C) placed in front of the beam expander. Although the

light beam is limited to 2 mm in diameter by the diaphragm, there exists light leakage around the ray caused by diffraction and scattering. In order to block this light leakage, quarter-wave plates (H, I) are inserted across the rays between the beam splitter and both reflectors. As each light beam passes the quarter-wave plate twice at the time of incidence and reflection, the phase difference between the ordinary ray and extra-ordinary ray becomes π. This means that the plane of polarization of the reflected ray becomes perpendicular to that of the incident ray. In such a way the returning light is cut off by the Glan-Thompson prism (A) and does not reach the laser.

4.5. Falling Object

The rotation of a reflector during its fall causes the shift of the returning point of the reflected ray. This shift makes a serious error in the length measurement. Some mechanical design is necessary to be able to drop the falling object with as little rotation as possible to minimize this phenomena on the reflected ray. At the same time, it is also necessary to give an optical character so that the parallelism between the incident ray and the reflected ray is kept in spite of the inevitable small rotation of the falling body.

A cubic corner prism or mirror is often used as a retroreflector having the optical character mentioned above. However, it has the following disadvantages. It's optically ineffective area is considerably large because the portions along the edge of each reflecting surface have to be avoided. A cubic corner has another disadvantage. Some additional mass has to be attached to the opposite side of its apex in order to make its center of gravity coincide with its apex. Because the optical path length along a ray is equal to the length of the line which is parallel to this ray and goes directly to its apex. The dimension of the instrument becomes large because of these disadvantages in using a cubic corner. One of the conditions necessary for the instrument is transportability. Taking such a condition into account, another optical system, the so called 'cat's eye', was adopted instead of cubic corner. This optical system has a mirror at the focus of an entrance convergence lens. The parallelism between incident and reflected rays, in spite of the rotation of the system, is kept as illustrated in Fig. 4-5. The invariance of the optical path length with the rotation at any point on the optical axis can be realized by adopting a suitable curvature of the reflecting surface (MOROKUMA, 1962). The shape of the cat's eye adopted is cylindrical, 33 mm in length and 20 mm in diameter and the weight is about 23.8 g.

The drop of the falling object has to be realized under no effect other than gravity. For this purpose, the coating of the electrical conductor

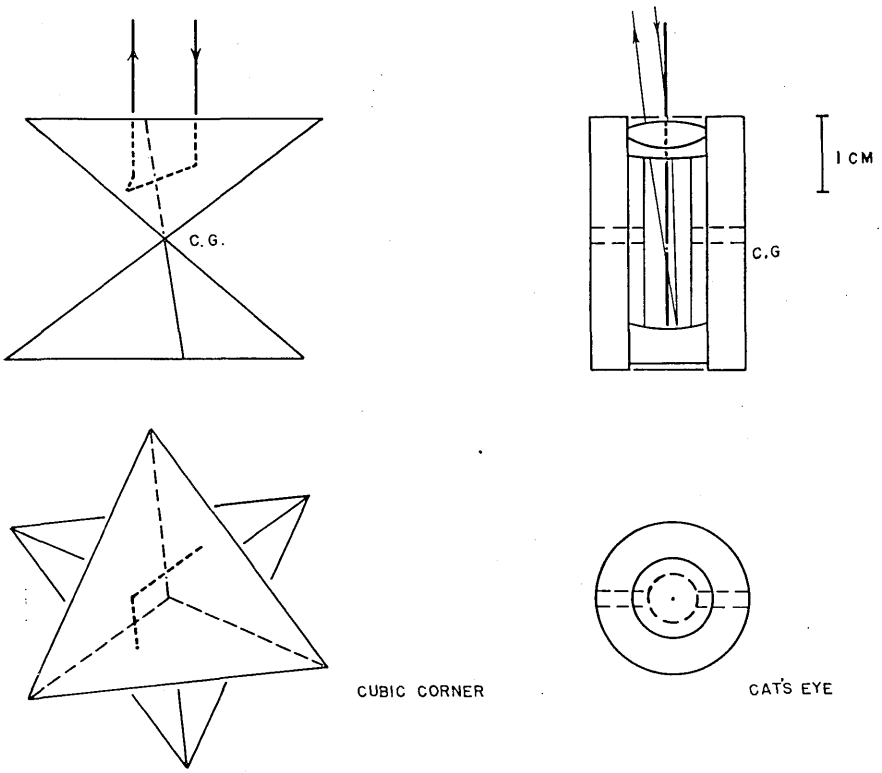

Fig. 4-5. Cubic corner prism and cat's eye.

is applied to the whole surface of the falling body to discharge electrostatic charge. Electric resistance between the upper and lower ends of the body is about 2 kΩ. The setting of the falling object to the starting position makes electric conductivity to the ground through the supporting beam and the vacuum chamber. Thus, the discharge of the electrostatic charge to the ground can be accomplished automatically before dropping. As for the effect of residual gas, it will be studied later.

4.6. Recording System

The present instrument employs a unique process in recording the falling distance in which a number of instantaneous positions during a single drop are recorded. The observation of the falling distance by such a method makes it possible to detect the details of the relative motion between the interferometer and the falling object. In other words, the vibrations of the interferometer, which reflect ground microtremors and mechanical vibrations of the instrument triggered at the start of the falling object, can be recorded. The effect of vibrations can be eliminated

by data processing, so that the instrumental protection against such vibrations is unnecessary. Hence the structure of the instrument can be made simple and it is convenient for field uses as a portable type.

The block diagram of the recording system is shown in Fig. 4-6. The specifications of the system are:

Falling distance	30 cm,
Wavelength	633 nm,
Sampling interval of falling distance	1 ms,
Display time for interference fringe	1 μs.

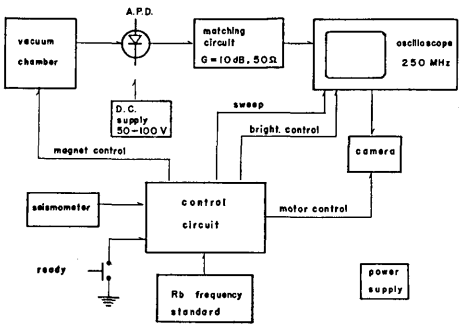

Fig. 4-6. Recording system.

Since the falling distance in the present instrument is set at 30 cm, the maximum falling velocity is about 2.42 m/s. The wavelength of a He-Ne laser is about 633 nm, hence the frequency of the interference fringe at the maximum speed reaches 7.5 MHz. If a relative accuracy of 1×10^{-8}, 10 μGal in gravity, is required, the falling distance has to be measured with an accuracy of 1×10^{-8}. In the case that a falling distance is measured by counting the numbers of the interference fringes of a 633 nm wavelength light, the phase angle measurement of the fringe should be made with an accuracy of a hundredth of a single fringe to ensure the required accuracy on the result, because the total number of fringes amounts to 950 000 for 30 cm falling distance.

Interference fringes are displayed on an oscilloscope and their photographs are taken. The intensity of the output light of the interferometer is converted to an electric signal by an avalanche photodiode. The electric signal is fed to the vertical axis of the oscilloscope after passing through an impedance matching circuit. Electronic circuits including the matching circuit are made as simple as possible to avoid signal distortion.

As for the time signal, a 100 kHz sine wave from a rubidium frequency standard is utilized. In the control circuit a sawtooth wave is generated. It has the repeating frequency of 1 kHz and the duration time of 1 μs, and is used as an input of the time axis of the oscilloscope. The sweep circuit prepared in the oscilloscope is not used to ensure timing accuracy. Thus the interference frings are displayed every 1 ms with a sufficient accuracy and the accurate correspondence between the falling time and distance is obtained. The display time of 1 μs in each sample interval of 1 ms makes several cycles sine wave patterns of the inter-

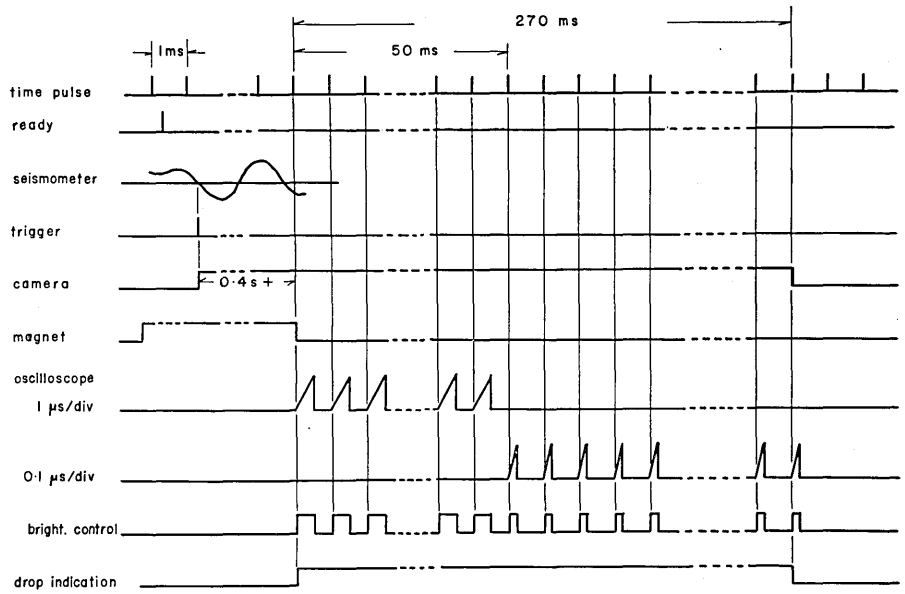

Fig. 4-7. Time sequence of recording.

ference fringes in the main part of 30 cm falling distance. But the oscilloscope receives no signal in the remaining hold off time of 999 μs. In other words, only 0.1 per cent of total fringe during a single drop is recorded. A recording photographic film is shifted in a camera during the no-signal time of 999 μs and is prepared for the next display. The spacing of displays on the film is 2 mm because the film runs in the camera at a rate of 2 m/s. Therefore, the sweep direction of the display of the oscilloscope is taken to the widthwise of the film to record the displayed fringe patterns within 2 mm length. As the film must run horizontally from the mechanics of the camera, the oscilloscope is placed in a style with the side way up. The frequency of interference fringe just after release of the falling object is not so high. As the display time is 1 μs, the displayed fringe patterns do not form a complete sine wave before their frequencies reach 1 MHz. It takes about 32 ms for the fringe frequency to reach this value. The present recording system has been revised so as to observe the detailed motion at the first stage of drop by lowering the displaying speed down to 1/10, i.e., 10 μs display time for the first 50 ms. Fringe patterns on the photographs are read by an X-Y coordinate digitizer.

The ground vibrations are believed to be one of the most serious disturbing factors. A long period vertical seismometer monitors ground motions and sends the starting signal to drop the falling object to the

recording system at the moment when the disturbance of ground motion to the result becomes minimum. Then the recording process starts automatically. Fig. 4-7 shows the recording sequence. Usually the reference point of interferometry has to be fixed in gravimetry. Much effort has been paid to this point in other studies. For instance, Faller adopts inertial suspension of the reference mirror and Sakuma cancels the ground vibrations by using piezoelectric elements as a suspender of the interferometer. In the present instrument, on the other hand, the absolute fixation of the reference point is not always necessary. The relative velocity of the reference point to the earth does not affect the obtained gravity value so long as the velocity is constant. Consequently, the protection against the ground motion becomes easy. This merit of the present instrument comes from the continuous recording of falling distance and the method of data processing. It will be explained later in Chapter 6. It can be said that the present instrument is sensitive only to an acceleration.

5. Observation

5.1. Preparation (on the optical system)

The apparatus was designed so as to be able to be easily disassembled for the convenience of transportation to an observation site and to be easily adjusted after reassembling. The adjustment of the optical system is aimed at realizing the plumbline direction of the descending light beam from the beam splitter to the falling object and securing a sufficient separation between the incident and reflected rays in association with the problem of the back talk of a laser as mentioned in Section 4.4. A little caution is necessary concerning the adjustment of the ray to the plumbline direction because of the slight inclinations of optical components through which the ray passes. The adjustment is carried out by making a coincidence between two images in a collimetor which is placed above the interferometer. One of these images is formed by the reflected ray from the fixed mirror of the interferometer and the other is formed by the reflected ray from the surface of a mercury pool which is put at the bottom of the instrument temporally. The coincidence of the two images at the realization of the true vertical of the ray is easily understood by the following optical conditions. The constant parallelism between the incident and reflected rays of a cat's eye, and the fact that the parallelism between the incident and reflected rays on the surface of a mercury pool is realized only when the incident ray passes in the true vertical direction. If deviation of incident ray from the vertical direction is θ

($\ll 1$), its effect to the measured falling distance becomes $\theta^2/2$. It is enough that this deviation angle is smaller than 28″ in order to secure an accuracy of 1×10^{-8} in the gravimetric result. The deviation causes the systematic errors by which we take the falling distance to be a little shorter, so that it is better to make such a deviation as small as possible. The optical system is adjusted so that the deviation is smaller than 5″ in the present instrument.

A falling object is set on the carriage in the vacuum chamber through the window on the chamber wall. It takes about two hours to reach an observable degree of vacuum after the evacuation begins. Loading of the camera and the electronic circuit check are carried out during this time.

5.2. Process of Observation

The processes of observation are outlined as follows.

1) The carriage ascends to set the falling object in the starting position.

2) The falling object is held by a catch, and then stays at the initial position independently of the descending of the carriage.

3) The carriage begins to descend.

4) The supporting beam for the falling object, which has been hung before the descending of the carriage, is risen to the horizontal position by the motion of the carriage through an escapement lever. The holding magnet fixes the supporting beam at the starting position.

5) The carriage descends to reach the bottom of the chamber.

6) The wavelength of the laser beam is set to the bottom of the Lamb dip by adjusting the space of the optical resonator. This is done manually to adjust the voltage, which is supplied to a piezoelectric element on which one of the resonator mirrors is fixed, monitoring the output intensity of laser light.

7) The degree of vacuum is read by an ionization gauge.

8) An avalanche photodiode is activated and the degree of interference is checked.

9) The seismometer starts recording.

10) A 'ready' signal is sent manually to the control circuit when all the check points are confirmed to be ready.

11) When the trigger signal is transmitted from the seismometer to the control circuit, the camera starts and finally the falling objects drops.

12) The seismometer recording stops and the power supply to the avalanche photodiode is cut off.

13) Consumptions of recording film is checked.

A Kodak tri-X 35 mm film (TX-402) is used for recording. The recorded film is developed by Pandol (a pirazon developer) for 15 minutes at a temperature of 20°C. The developing time is prolonged from the normal 4 minutes to 15 minutes because of the feebleness of the oscilloscope display.

6. Data Processing

The equation of motion of a falling body under the uniform gravity field is represented as:

$$m\frac{d^2x}{dt^2}=mg \tag{6-1}$$

where m is the mass of a falling body, x, the falling distance taken its axis vertically downward, t, the time and g, the acceleration due to gravity. When the initial conditions at $t=0$ are $x=x_0$ and $dx/dt=v_0$, then

$$x=\frac{1}{2}gt^2+v_0t+x_0. \tag{6-2}$$

The value of gravity, g, is taken as a constant here. The effect of the vertical gradient, i.e., the gravity difference with height will be treated later.

If the falling distance is measured succesively at a constant sampling rate of Δt during a single drop, a sequence corresponding to the increasing falling distance is obtained. Another sequence composed of the second difference of the sequence of the falling distance has a remarkable character. Each term of this sequence, $\Delta''x_i$, is constant and has value given by $\Delta''x_i=g(\Delta t)^2$, $(i=2, 3, 4, \ldots, n-1)$ regardless of the initial position x_0 and the initial velocity v_0. $\Delta''x$ becomes 9.8 μm because the sampling interval Δt is 1 ms in the present instrument. It corresponds to about 30.96 $(=\Delta''x/(\lambda/2))$ in fringe units in the interference of a 632.9 nm wavelength light.

As mentioned before, the records on film are in fringe patterns during 1 μs at intervals of every 1 ms. Strictly speaking, each fringe pattern of a sine curve does not form an accurate sine curve, because it reflects a motion of uniform acceleration, but not that of a constant velocity. However, the discrepancy between the fringe pattern and an accurate sine curve is very slight. The phase difference is given by gt^2/λ and this value is estimated as only 1.55×10^{-5} after 1 μs time interval. The reading accuracy of the phase angle on the record is estimated to be in the order of 10^{-2} fringe, thus, it is permissible to take the assumption that a falling

body drops with a constant velocity and hence the fringe patterns form accurate sine curves during 1 μs of each sweep time. An example of a recording is shown later in the forthcoming chapter.

The following formulas are applied to each trace of the fringe pattern,

$$y=a_i \sin(\omega_i t+\theta_i)+b_i t+c_i, \qquad (i=1, 2, 3, \ldots, n) \tag{6-3}$$

where i is the trace number, t, time, y, change in the intensity of fringes, a_i, amplitude, ω_i, angular frequency, θ_i, initial phase angle ($0 \leq \theta_i < 2\pi$), b_i, inclination of the trace axis, c_i, constant depending on the distance between the trace axis and the origin of y and n, numbers of trace. a_i, ω_i, θ_i, b_i and c_i are determined by the least squares method using the successive approximations. Time, t, on respective traces are taken as in different time systems from each other and their origins are set at the beginnings of the respective traces. It is a matter of course that the time interval between neighbouring time systems is 1 ms with an accuracy of 1×10^{-11}.

Let ϕ_i ($\equiv \theta_i/2\pi$) be the phase of each trace at the origin of the respective time systems. Then a sequence of second differences $\Delta''\phi_i$ ($i=2, 3, 4, \ldots, n-1$) is calculated from the sequence of ϕ_i as is shown in Table 6-1. Each term of this sequence of the second difference should have an approximate value of 0.96, taking its fractional part, since the second difference must be approximately 30.96. This is the expression of a fractional part of a sequence of the actual fringe count. The new sequence which is obtained by adding the value of 30 (or 31) to each term coincides with the actual sequence accompanying a drop of the falling object. Actually, the phase corresponding to the central grid line of the oscilloscope is calculated, instead of the initial phase so as to be able to compare it directly with a comparator reading of trace in the case of such a necessity.

Arbitrary values are assumed as the first and second terms of the sequence of fringe count, and then the complete sequence of fringe counts corresponding to each sampling time is obtained from these assumed initial values with the sequence of the second differences of fringe counts through the inverse process. The assumption of the initial fringe counts, the first and the second terms, is equivalent to an assumption of the first term and the difference between the second and the first terms of the fringe count. That is to say, it is equivalent to assuming the initial position x_0 and the initial velocity v_0 of the falling object. This assumption does not affect the result of the measuring of the gravity value at all.

The following formula is fitted next to this sequence of composed fringe counts by the least-square approximation,

Table 6-1. Fringe count construction.

Trace No.	Phase	Δ'	Δ''	$30(31)+\Delta''$	Fringe count
1	0.84				0.84
2	0.78	( ).94	( ).95	30.95	15.78
3	0.66	( ).89	( ).97	30.97	61.66
4	0.52	( ).86	( ).96	30.96	138.52
5	0.33	( ).81	( ).95	30.95	246.33
6	0.09	( ).76	( ).95	30.95	385.09
7	0.80	( ).71	( ).94	30.94	554.80
8	0.45	( ).65	( ).97	30.97	755.45
9	0.07	( ).62	( ).96	30.96	987.07
10	0.66	( ).58	( ).99	30.99	1249.66
11	0.23	( ).57	( ).93	30.93	1543.23
12	0.74	( ).50	( ).99	30.99	1867.74
13	0.23	( ).49	( ).95	30.95	2223.23
14	0.67	( ).44	( ).93	30.93	2609.67
15	0.04	( ).37	( ).97	30.97	3027.04
16	0.37	( ).34	( ).91	30.91	3475.37
17	0.62	( ).25	( ).01	31.01	3954.62
18	0.88	( ).26	( ).90	30.90	4464.88
19	0.04	( ).16	( ).01	31.01	5006.04
20	0.21	( ).17	.	.	5578.21
.	.	.	.	.	.
.	.	.	.	.	.
.	.	.	.	.	.

$$x=At^2+Bt+C. \tag{6-4}$$

The gravity value, g, is easily calculated from the obtained value of A.

As is easily understood from the above explanation, the direct count of interference fringes is quite unnecessary for the measurement of falling distance in this system. The only necessary process of fringe recording is the cathod ray tube display at a constant rate. Thus the recording system is quite simple. This is one of the unique points of the instrument. Phase shift in the electronic circuits due to increase in the frequency of the interference fringe is not so serious that it can be neglected. As for the phase shift, it will be treated in Section 7.9.

After fitting sine curves to each fringe pattern, the residuals have no distinct tendency with the increase in frequency as shown in Appendix I, so that equal weights are applied to each fringe count in the fitting (6-4).

It is worth while to mention that it is theoretically possible to estimate the actual effect of residual gas resistance on the motion of a fall-

ing object. In order to do this, the accurate initial velocity must be known. The equation of motion of a falling body under the gravity and gas resistance is given by

$$m\frac{d^2x}{dt^2}=mg+kv, \tag{6-5}$$

where k is the coefficient of resistance. A linear relation between velocity, v, and resistance will be confirmed later. As $v=gt+v_0$, the following relation is obtained.

$$x=\frac{1}{6}\frac{kg}{m}t^3+\frac{1}{2}\left(g+\frac{kv_0}{m}\right)t^2+v_0t+x_0. \tag{6-6}$$

It is understood from the above relation that if a time function of a third power is fitted to x, we can obtain the value k from the coefficient of the t^3-term. The combination of k with v_0 makes it possible to apply a correction for resistance to the obtained gravity value from the coefficient of the t^2-term. If the origin of time is choosen so as to let $v_0=0$, by replacing t by $t+\Delta t$ $(=v_0/g)$, it looks like the correction becomes zero. But it goes without saying that the alternative t^2-term by the expansion of the t^3-term, as $kg(t+\Delta t)^3/6m=kgt^3/6m+\underline{kgt^2\Delta t/2m}+\cdots$, gives the same effect, because $g\Delta t=v_0$ in this case. Note that the time system is given at the time of the recording of the falling distance independently of v, consequently it is not always possible to take the time system as $t=0$ at $v_0=0$. Taking this theoretical possibility on the resistance correction into account, the sweep time of the oscilloscope is prolonged to 10 μs for the first 50 ms of a drop to obtain the detailed information about the initial velocity.

7. Disturbing Factors

There are many disturbing factors as probable sources of systematic and random errors in the absolute measurement of gravity by means of a free fall method. The gravity values obtained may contain errors due to the following sources:

1) Inaccuracy in the wavelength of laser light
2) Inaccuracy in the time derived from a frequency standard
3) Finite velocity of light
4) Vertical gradient of gravity
5) Resistance of residual gas
6) Deviation of the ray from the vertical direction
7) Inaccuracy in manufacturing a falling object and its inclination during drop

8) Electric and magnetic forces
9) Delay of electric signal in electronic circuits
10) Temperature effect
11) Instrumental oscillation.

These factors will be treated in the following sections in detail.

7.1. Wavelength of Laser

As a falling distance is measured with the laser wavelength as a scale, its inaccuracy affects directly the results. As mentioned in Section 4.4., the accuracy of 1×10^{-8} in wavelength is required in order to obtain the accuracy of 0.01 mGal in the result. The laser employed for this work is the JLG-HS6 made by the Japan Electron Optics Laboratory Co., Ltd., the original type of which had a conventional system of servo loop to set the wavelength into the Lamb dip and the guaranteed accuracy in this state is 1×10^{-8}. This laser barely satisfies above requirement.

7.1.1. Resettability

The laser in its original style has an accuracy of 1×10^{-8}. However, the setting of the wavelength to the bottom of the Lamb dip is manually made at each drop as mentioned before, therefore, the resettability must also be investigated. Here, 'resettability' means the degree of coincidence in wavelength when the oscillation state of a laser is set repeatedly. The change in wavelength with the variation in the distance between two resonator mirrors is simply estimated as follows. The oscillation condition repeats with every $\lambda/2$ change of mirror distance, in other words, the shift of the oscillation condition from a Lamb dip to the neighbouring Lamb dip corresponds to a $\lambda/2$ change in the distance of the mirrors (b, c in Fig. 7-1). If the distance between two mirrors is increased gradually by $\lambda/2$ from a Lamb dip to the next, the following occurrs, the wavelength increases by $d\lambda$ with the first half shift of a mirror of about $\lambda/4$, and jumps down

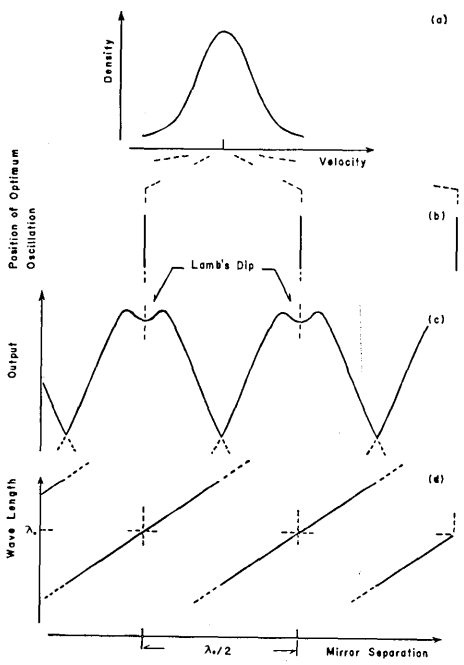

Fig. 7-1. Lamb dip.

some amount at the middle of the shift motion and then recovers its original length at the next Lamb dip with the latter half shift (d in Fig. 7-1).

The relation between the distance of the resonator mirrors s and the wavelength λ is

$$s=\frac{q\lambda}{2}, \tag{7-1}$$

where $q=[2s/\lambda]$, the nearest integer to $2s/\lambda$, so that we have

$$d\lambda=\left(\frac{q}{2}\right)ds. \tag{7-2}$$

Leting $\lambda=633$ nm, $s=20$ cm, we then get $q=6.3\times10^5$ and the change in the wavelength corresponding to $ds=\lambda/2$ is about 1×10^{-3} nm, so that we have $d\lambda/\lambda=1.6\times10^{-6}$. This means that the distance of the mirrors has to be set with an accuracy of 6.25×10^{-3} (=required accuracy/relative wavelength shift with a mirror shift from a Lamb dip to the next dip) of the full shift between two consecutive Lamb dips to keep the equation, $dg/g=d\lambda/\lambda=1\times10^{-8}$. This requirement is rather difficult to satisfy, and thus the resettability of the wavelength of the laser is one of the limiting factors in the present instrument.

It is certain that an iodine stabilized He-Ne laser will become available in near future and will remove the uncertainty on the length measurement in the absolute measurement of gravity (WALLARD et al., 1975).

7.2. Time Standard

As $dg/g=-2(dt/t)$, the timing accuracy of 5×10^{-9} is required to make a measurement of gravity with an accuracy of 1×10^{-8} by the free fall method. The time standard used has to keep at least the same accuracy. It is not difficult to realize such an accuracy in time even by using a crystal clock as long as the concerned period is short. A crystal clock, however, has a drift on its frequency inevitably, hence regular checks on its frequency are indispensable for long-term observations. As one of the purposes of constructing the instrument is to detect a secular change of gravity, the problem of the frequency check may become an obstacle to long-term observations. A rubidium frequency standard type 5065A of Hewlett-Packard Co. has been adopted as a time standard, because it has a long-term drift less than 1×10^{-11}/month. (Its short-term stability is far better: 5×10^{-13}/100 s.) This ensures a sufficient accuracy for the time measurement.

It is necessary for an absolute measurement of gravity to be free from the instrumental drift especially for the purpose of detecting the

secular variation in gravity. The measurement is meaningless if the true secular variation of gravity cannot be distinguished from the instrumental drift. Considering the absolute measurement of gravity by the free fall method results in the measurements of time and distance, it deserves a special emphasis that the present method is very suitable for detecting the secular variation in gravity, in which the drift-free quantum mechanics phenomena of transitions between energy levels: i.e., a rubidium frequency standard and a laser, are utilized.

7.3. Finite Velocity of Light

The travel time of light to and from a falling object increases with an optical path length during the drop of the falling object. It brings about a delay in the generation of interference fringes because it takes longer travel time for light in lower part of the drop owing to the increase of the optical path length, hence a correction is necessary.

Interference fringes can be regarded as a kind of beat signal resulting from the light frequency shift by the Doppler effect. Let the light velocity be c, the wavelength of light from a standing source λ_0 and the velocity of the falling object v, then, the frequency of reference light is given by

$$\nu_r=\frac{c}{\lambda_0}. \tag{7-2}$$

The falling object receives the incident light, the frequency of which is

$$\nu_d=\frac{c-v}{\lambda_0}. \tag{7-4}$$

The photodiode receives the reflected light from the falling object, being regarded as a moving source, the wavelength of which is

$$\lambda_s=\frac{c+v}{\nu_d}, \tag{7-5}$$

i.e., the frequency of the light received by the photodiode is

$$\nu_s=\frac{c(c-v)}{(c+v)\lambda_0}. \tag{7-6}$$

The interference fringe can be regarded as a beat wave between ν_r and ν_s, so that the wave count of the interference fringes dn is expressed in the term of the time interval dt as

$$dn=(\nu_r-\nu_s)dt=\left(\frac{c}{\lambda_0}-\frac{c(c-v)}{(c+v)\lambda_0}\right)dt. \tag{7-7}$$

The fringe count n during the falling time t is

$$n=\int_0^t \frac{c}{\lambda_0}\left(1-\frac{c-v}{c+v}\right)dt. \tag{7-8}$$

As $v \ll c$, then we have

$$n \fallingdotseq \frac{1}{\lambda_0}\int_0^t \left(2v-\frac{2v^2}{c}\right)dt, \tag{7-9}$$

and moreover, taking $v=gt$ into consideration, we have

$$n=\frac{1}{\lambda_0}\left(gt^2-\frac{2g^2t^3}{3c}\right). \tag{7-10}$$

If the falling distance s is simply calculated by multiplying $\lambda_0/2$ to the obtained fringe count, and the apparent gravity value g_a is calculated by the equations $s=(1/2)g_at^2$, then

$$g_a=\frac{2s}{t^2}=g-\frac{2g^2t}{3c}. \tag{7-11}$$

The correction $\Delta g=g-g_a=2g^2t/3c$ must be applied to the apparent gravity for eliminating an effect of the finiteness of light velocity. In the case of $t=0.25$ s, we then conclude

$$\Delta g=5.3\times10^{-8}\ \mathrm{m/s^2}=5.3\ \mu\mathrm{Gal}.$$

7.4. Vertical Gradient of Gravity

The vertical gradient of gravity is approximately 0.3 mGal/m. Since the falling distance in the present instrument is 30 cm, the difference in the gravity values at upper and lower ends of falling path amounts to about 0.1 mGal. Such a difference must be considered because the measuring accuracy is aimed at the order of 0.01 mGal.

If the x-axis is taken vertically downward from the starting position, the gravity value at the starting position g_0, and the vertical gradient of gravity k, then the equation of motion of a falling body is

$$m\frac{d^2x}{dt^2}=m(g_0+kx), \tag{7-12}$$

which has the solution expressed as

$$x=\frac{g_0}{k}\{\cosh(\sqrt{k}\,t)-1\}. \tag{7-13}$$

The falling body drops about 8 mm longer during 0.25 s in this case, com-

paring with the drop in the uniform gravity field of g_0.

As was explained in Section 6, the falling distance is calculated on the assumption of the uniform gravity, i.e., the constant second difference of falling distance. Strictly speaking, the second difference corresponding to the lower part of the falling path is 1×10^{-7} as large again as that of the upper part. The discrepancy of the second differences is of course not so large that the assumption of the constant second difference is considered to be reasonable. But the effect of the vertical gradient on the obtained result brings another problem up and it can not be neglected. As the obtained gravity value must be equal to the value at a position in the drop path, considering that it is an averaged value of increasing gravity along the drop path, the effect of the vertical gradient of gravity may be expressed by calculating the height where the gravity value is equivalent to the obtained gravity value.

Let a force acting on the falling object other than the constant gravity be $f(t)$ as a function of falling time t. Then the equation of motion of the falling object is represented as

$$m\frac{d^2x}{dt^2}=mg_0+f(t). \tag{7-14}$$

(7-14) is approximated as

$$m\frac{d^2x}{dt^2}=mg_m \tag{7-15}$$

on the assumption that the gravity value is constant g_m along the x-axis. The difference between g_0 and g_m is as follows. Let x according to (7-14) be x_1, and the corresponding x according to (7-15) x_2. x_1 is the actual falling distance under the real gravity field and x_2 is the virtual distance under the assumed constant field, so that

$$x_1=\frac{1}{2}g_0t^2+\frac{1}{m}\iint f(t)(dt)^2, \tag{7-16}$$

$$x_2=\frac{1}{2}g_mt^2. \tag{7-17}$$

The first order and constant terms on falling time t concerning the initial velocity and position may be neglected under the assumption of ideal drop. In the present work, g_m is determined as

$$\int(x_1-x_2)^2dt=\min. \tag{7-18}$$

Putting

$$\frac{1}{m}\iint f(t)(dt)^2 \equiv F(t),$$

then (7-18) becomes

$$\int\left(\frac{1}{2}(g_0-g_m)t^2+F(t)\right)^2 dt \equiv U=\min. \tag{7-19}$$

As we take

$$\frac{\partial U}{\partial(g_0-g_m)}=0,$$

finally we have

$$g_0-g_m=-\frac{2\int F(t)t^2dt}{\int t^4dt}. \tag{7-20}$$

In the case of the vertical gradient of gravity, $f(t)$ is expressed as

$$f(t)=\frac{1}{2}mkg_mt^2, \tag{7-21}$$

then, we get

$$F(t)=\frac{1}{24}kg_mt^4 \tag{7-22}$$

$$g_0-g_m=-\frac{5}{84}kg_mt^2. \tag{7-23}$$

Now letting h be the distance along the x-axis from the initial position to the point where gravity equals g_m, we have

$$g_m=g_0+kh \tag{7-24}$$

$$g_m-g_0=kh=\frac{5}{84}kg_mt^2. \tag{7-25}$$

We denote the total falling distance and time by H and T respectively, then, from (7-17), we have

$$H=\frac{1}{2}g_mT^2. \tag{7-26}$$

Substituting T into (7-25), we obtain

$$h=\frac{5}{42}H. \tag{7-27}$$

It can be said from (7-27) that the present method measures the gravity

value at the place lower than the top of drop trajectory by 5/42 times the drop path length.

SENDA et al. (1971) adopted 1/6 instead of 5/42 as a correction coefficient according to SAKUMA (1959). But the value 1/6 is applicable only when the following assumption is adequate. That is, the falling distance under the gravity field with a vertical gradient is equal to that under the uniform field in the same falling time regardless of the detailed relation between the falling distance and time in the drop. Such a correction coefficient cannot be applied to the present work in which the least square approximation is used for the data of the falling distance obtained by a constant sampling rate. The reason why the coefficient is smaller than 1/6 is that the data on upper part of the drop trajectory has a greater weight because it is denser in number than that of lower part of trajectory.

The instrumental height is variable according to the setting condition of the instrument at an observation site, hence the obtained gravity value should be reduced to ground level. This reduction is $\Delta g = ke$, where e is height of the position that the gravity value is equal to g_m in the drop trajectory above ground level. Since an average value of the height e for the present instrument is taken as 75 cm, Δg becomes about 0.23 mGal. As the vertical gradient of gravity depends on the local topographical and geological conditions, the value derived from observed data at a site should be adopted as k. It is difficult to maintain the accuracy of 0.01 mGal/m for k, although it is obtained from the measurement by a modern spring-balance type gravity meter. Consequently the practical accuracy of the correction for the instrumental height has been estimated to be 0.01 mGal or so. This uncertainty on k is one of the limiting factors to the accuracy of the obtained gravity value by an absolute measurement.

From the viewpoint of detecting a secular variation of gravity, the reduction of the measured gravity value to the ground level is not always necessary, because its direct comparison with the previous value is possible. But the setting of an instrument in the same conditions is not always possible, therefore, the reduction to the ground level is advisable. There is a way, other than the use of a gravity meter, for this purpose, that is, to develop a special instrument measuring dg/dz directly. The measurement of dg/dz itself is an important theme and it also works for improving the accuracy of the absolute measurement of gravity.

7.5. *Residual Gas*

Residual gas in the falling chamber works as a resistant substance against the motion of the falling object, however, it is not advisable in

constructing the instrument to pay much attention to realizing too low gas pressure. Accordingly, the estimation of the degree of vacuum which gives no appreciable effect to the gravity measurement must be carried out.

The principle of the method of estimating the effect of residual gas has already been reported by COOK (1957). It may be assumed that pressure inside the falling chamber is so low that Knudsen gas regime is realized. The mean free path of a gas molecule is longer than the characteristic size of the chamber and mutual interactions of gas molecules become negligible. This indicates that the residual gas works effectively as collision particle against the falling object. Molecules of residual gas may be regarded as having a random component in their velocity.

Some of molecules collide against the falling object, and as their velocity distribution is random, the number of colliding particles obeys the cosine law. Molecules which collide against the falling object are reemitted from its surface according to the same cosine law relative to the falling object (FRENKEL, 1924; HURLBUT, 1957). This means that reemitted particles have a mean velocity which is equal to the velocity of the falling object relative to the vacuum chamber. The incident particles acquire some momentum from the falling object at collision. This process works as a resistance against the motion of the falling object.

Letting the mean velocity of reemitted gas molecules be U, which is equal to the velocity of the falling object as mentioned before, the momentum loss of a falling object per unit time (momentum loss rate) is

$$\Delta\dot{p}=nmU, \tag{7-28}$$

where m is the mass of gas molecule and n, the number of molecules which are reemitted from the falling object per unit time. n is written as

$$n=\frac{1}{4}A\nu\bar{v}, \tag{7-29}$$

where A is the surface area of a falling object, ν, the number density of gas molecule and $\bar{v}$, the mean velocity of the gas molecule. Thus $\Delta\dot{p}$ can be expressed by

$$\Delta\dot{p}=\frac{1}{4}A\nu\bar{v}mU. \tag{7-30}$$

The velocity distribution of incident molecules cannot be regarded as completely random and some amount of the momentum taken out is given back to the falling object, because a part of the reemitted molecules returns to the falling object by collision with other particles without any interaction with the wall of the vacuum chamber. Taking such an

effect into account, the related momentum loss rate may be somewhat smaller. In the case of the absolute measurement of gravity, the effect of residual gas must be negligibly small, even at its maximum.

The falling object has a cylindrical shape with a height of 33 mm and a diameter of 20 mm, then the surface area A is 2.70×10^{3} mm^2, and the mean velocity of the molecules $\bar{v}$ is taken as

$$\bar{v}=\sqrt{\frac{8kT}{\pi m}}=462.9 \text{ m/s}, \tag{7-31}$$

where k is Boltzmann's constant ($=1.380662\times10^{-23}$ J/K), T, temperature ($=293.15$ K) and m, the mass of the gas molecule whose molecular weight is taken as 28.96 ($=4.809\times10^{-26}$ kg).

The effect of the residual gas is maximum at the lower end of the falling trajectory where the falling velocity is maximum. Hence it is enough, if the effect of residual gas at the lower end is smaller than the measuring accuracy of gravity. According to (7-30), the maximum momentum loss rate for the final falling velocity ($U=2.42$ m/s) is

$$\Delta\dot{p}=3.639\times10^{-26}\nu \text{ kgm}^4/\text{s}^2. \tag{7-32}$$

The acceleration of the falling object due to the momentum loss can be obtained by dividing this momentum loss rate by its mass M. If the following condition is attained, the maximum effect of the residual gas does not exceed 0.01 mGal.

$$\frac{\Delta\dot{p}}{M}=1.529\times10^{-24}\nu \text{ m}^4/\text{s}^2<1\times10^{-7} \text{ m/s}^2. \tag{7-33}$$

From this condition, we obtain $\nu<6.540\times10^{16}$ m^{-3}, that is, the pressure P in the vacuum chamber must be $P<2.646\times10^{-4}$ Pa ($=1.985\times10^{-6}$ Torr), or the relation between the degree of the vacuum P and its maximum effect Δg on the measured gravity is roughly represented as

$$\Delta g=4\times10^{1}P \text{ mGal/Pa} \quad (=5\times10^{3}P \text{ mGal/Torr}). \tag{7-34}$$

More generally, the total effect of the residual gas during the drop of a falling object can be treated as follows. The momentum loss rate of the falling object, in other words, the force exerted by the residual gas on the falling object, is represented as

$$\Delta\dot{p}=f=\frac{1}{4}A\nu\bar{v}mU=3.716\times10^{-6}PU \text{ Ns/Pam}$$
$$=4.954\times10^{-4}PU \text{ Ns/Torrm}. \tag{7-35}$$

The difference between the gravity values obtainable in a complete vacuum

and in a condition with residual gas, which are denoted by g_0 and g_m, respectively, is calculated according to the discussion in Section 7.4.

$f(t)$ in (7-14) is, for the present case,

$$f(t)=-3.716\times10^{-6}\,PU \text{ Ns/Pam}, \tag{7-36}$$

and

$$U=gt.$$

With the falling time t, we obtain

$$F(t)=\frac{1}{M}\iint f(t)(dt)^2=-6.193\times10^{-5}\frac{Pgt^3}{M} \text{ Ns/Pam}. \tag{7-37}$$

Finally, we have

$$g_0-g_m=-\frac{2\int F(t)t^2dt}{\int t^4dt}=1.032\times10^{-6}\frac{PgT}{M} \text{ Ns/Pam}, \tag{7-38}$$

where T is the total falling time.

For the present instrument, we take $M=2.38\times10^{-2}$ kg, and $gT=U_{\max}=2.42$ ms^{-1}, so that we have

$$g_0-g_m=1.05\times10^{1}P \text{ mGal/Pa}=1.4\times10^{3}P \text{ mGal/Torr}. \tag{7-39}$$

For example, $g_0-g_m=7\times10^{-3}$ mGal when $P=5\times10^{-6}$ Torr.

7.6. Deviation of the Direction of Ray from the Vertical

If the direction of the incident ray to the falling object deviates slightly from the vertical by θ, the falling distance is underestimated by a factor of $\cos\theta$. Then the relation between the true falling distance S and the apparent falling distance S_a is

$$S_a=S\cos\theta. \tag{7-40}$$

The difference between the true gravity g and the apparent one g_a, which is derived from the same relation $S=(1/2)gt^2$, as in g, is

$$\Delta g=g-g_a=\frac{2S}{t^2}-\frac{2S_a}{t^2}=(1-\cos\theta)\frac{2S}{t^2}. \tag{7-41}$$

Usually $\theta\ll1$, so that (7-41) becomes

$$\Delta g=\frac{1}{2}g\theta^2. \tag{7-42}$$

For example, when $\theta=10''$ $(=5\times10^{-5})$, then the difference is 1.2×10^{-3} mGal.

7.7. Falling Object

In the free fall method, the falling distance can be calculated on the assumption that the falling object is equivalent to a point mass. In the strict sense, however, such an assumption can not reflect actual physical conditions which sometimes exceed a tolerable limit. Among the factors disturbing the measured falling distance, the optical path length change due to the rotation of a falling object may be the most serious. This kind of problem will be treated in this section. The minimum of rotation will first be investigated and the discussion about the optical path length change will come next.

7.7.1. Rotation of a Falling Object

Possible causes of the rotation are considered here. The supporting beam, on which a falling object is set, is pivoted at its one end (tail) and is supported horizontally by an electric magnet at its head. The supporting beam bends downward due to the weight of a falling object and the pressure of a start spring. The beam begins to vibrate in the transverse form at the moment the magnet releases the supporting beam. Contact between the supporting beam with the falling object is interrupted by such transverse vibration. It is obvious, taking the propagation velocity of the vibrations into account, that there is a very small time lag in which one contact (gold boss) is detached from the falling object, but the other gold bosses are still in contact during the propagation period of the transverse wave from head to tail of the supporting beam. The falling object gains rotation velocity by the gravity moment during this time lag. This can be considered as a cause of the rotation of the falling object.

The supporting beam can be approximated as a rectangular bar of duralumin. Its dimension is as follows; length is 53 mm (separation between the pivot and the magnet), thickness 3.8 mm, width 1 mm (head) and 2.5 mm (tail). Though its width varies from head to tail, such a variation does not affect k (see below for the meaning of k), so that it can be disregarded. The oscillation frequency, ν_s, of the transverse vibration of the rectangular bar in the case of one end support is represented as

$$\nu_s=\frac{m_s^2 k}{2\pi l^2}\sqrt{\frac{E}{\rho}}, \tag{7-43}$$

where m_s is the degree parameter ($=1.875$), k, the radius of gyration which is determined from the moment of inertia of the cross-section about an axis through its center at a right angle to the plane of bending ($=1.097\times10^{-3}$ m), l, the length of the bar ($=5.3\times10^{-2}$ m), E, Young's

modulus ($=7.17\times10^{10}\,\mathrm{Nm^{-2}}$) and ρ, the density ($=2.79\times10^{3}\,\mathrm{kgm^{-3}}$). We have $\nu_s=1108\,\mathrm{Hz}$. As the beam vibrates in such a way that one end is free and the other end is supported, its wavelength is taken as $\lambda=4l=2.12\times10^{-1}\,\mathrm{m}$. The pattern of oscillation in this case is that of a standing wave, which is usually regarded as a composition of two travel waves having mutually reverse propagation directions but the same amplitudes. It may be considered that one of these travel waves starts first at the beginning of the initial moment of vibration and this is the propagation of the transformation of the supporting beam along its axis. The velocity of this wave is $v=\nu_s/4l=234.8\,\mathrm{ms^{-1}}$. The distance, d, between the gold bosses which support the falling object along the length of the supporting beam is $1.125\times10^{-2}\,\mathrm{m}$. The travel time, t, of the vibration wave across this distance is $t=d/v=4.79\times10^{-5}\,\mathrm{s}$. The moment of inertia of the falling object I around the point of support is estimated to be $9.88\times10^{-7}\,\mathrm{kgm^2}$, and the moment L due to gravity exerted on the falling object is $L=8.45\times10^{-4}\,\mathrm{Nm}$. Then, the rotation velocity ω of the falling object becomes $\omega=Lt/I=4.1\,\mathrm{rads^{-1}}$ during this supporting time. The total angle of rotation θ during the falling time T ($=0.25\,\mathrm{s}$) is $\theta=\omega T=1.025\times10^{-3}\,\mathrm{rad}$ ($=3.5'$). Consequently, it is concluded that the change in optical path length of an optical system of a falling object due to the rotating angle of 3.5′ should be so small if the aimed accuracy of the measurement of gravity can be attained without any consideration of the rotating effect.

7.7.2. Optical Characteristics of a Falling Object

As mentioned in Section 4.5., the curvature of the reflecting surface of the falling object so called cat's eye has been so designed that the optical path length is insensitive to change in the inclination of the falling object. It has been determined according to the following formula (MOROKUMA, 1962),

$$\rho=\frac{f^2}{r+k+2f} \tag{7-44}$$

where ρ is the radius of curvature of reflecting surface, f, the focal length of the lens, k, the distance between first and second principal points of the lens, and r, the distance between the reflecting surface and the center of rotation. However, the constancy of the optical path length with change in inclination of the cat's eye holds only in the case of a paraxial ray, and the optical path length changes when the falling object inclines by a finite angle. Manufacturing inaccuracy, i.e., deviation from its optical design, also may seriously influence the optical characteristics of the falling object. These effects on the relation between the tilt of a cat's eye and the variation in an optical path length are cal-

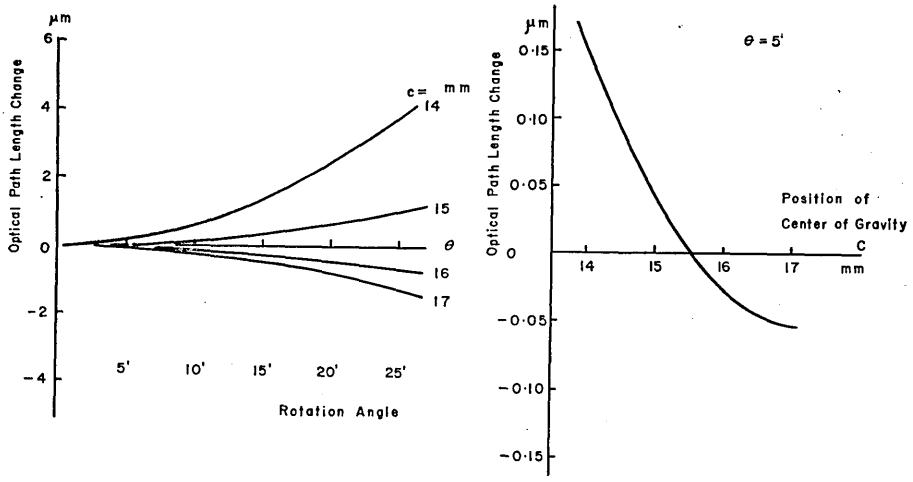

Fig. 7-2. Optical characteristics of a cat's eye.
left: Optical path length change versus tilt angle of a cat's eye. Parameter c represents the position of its mass center measured from its upper end.
right: Optical path length change versus position of the mass center when tilt angle is 5′.

culated by ray-tracing with the following parameters: the curvature of a reflecting surface, the distance between a lens and a reflecting surface and the position of the rotation center. Fig. 7-2 shows a typical example of calculated results.

According to these results, the variation in an optical path length is insensitive to the distance between a lens and a reflecting surface and its discrepancy of 0.1 mm from the designed value does not bring about a change in the optical path length exceeding 1.7 nm for 5′ tilt of the cat's eye. On the other hand, inaccuracy in the position of the rotation center, that is, the center of gravity, affects considerably the optical path length change with rotation. For example, change of 0.1 mm in the position of the rotation center along its optical axis may cause a 7 nm change in the optical path length for the same inclination angle of 5′. Since the change in the optical path length, with a constant rate inclination of a falling cat's eye, behaves as a type of parabolic function of time, there is no way to separate this effect from obtained gravity values. This means, that if a falling object, whose center of gravity is 0.1 mm out of planned position, tilts by 5′ during dropping, the rotation may cause an error in gravity amounting to 22 μGal. If a falling object has an ideal axial symmetry in its structure and if it is set exactly vertically at the starting position, this kind of error may become systematic. Such ideal conditions, however, can not be actually

realized and the corresponding effect on observed gravity values can be positive or negative according to the initial orientation of a falling object and its direction of tilt. So this effect may be treated as one of the sources of random error rather than systematic, provided its orientation at the starting position and direction of tilt during its drop are both at random.

7.8. Electric and Magnetic Effects

Electric and magnetic effects on the motion of a charged falling object are considered in this section. These effects affect directly the motion in the gravity field. As a ferromagnetic material is not utilized for both the falling object and the vacuum chamber, except for the pole piece of the holding magnet for the supporting beam on which the falling objects is set before the drop, it is thought that the static magnetic force may give no significant effect. As mentioned in Section 4.5., the surface of a falling object has electric conductivity, and as the electric circuit is made to the ground through the handling devices before the drop, no electrostatic charge remains on the falling object before its start. But a small amount of electric charges appears on the falling object at the moment of it's start because of the contact potential difference between the chromium-plated bottom surface of the falling object and the gold bosses of the supporting beam.

Letting electric capacitance, formed between the falling object and the vacuum chamber including the inside frame, be denoted by C, then, appearing electrostatic charge will be represented by $Q=CV$, where V is the contact potential difference between gold and chromium. An estimation of the electric capacitance is so tedious that the calculation process is omitted here. The result of the calculation gives $C=6.6\,\mathrm{pF}$. The contact potential difference is equal to the difference of the work functions of gold and chromium. The work function of chromium is unknown, so that the contact potential difference is overestimated to be 1 V. The electrostatic charge remaining on the falling object in the course of it's drop is consequently estimated to be $6.6\times10^{-12}\,\mathrm{C}$.

The electrostatic charge affects the motion of a falling object through Coulomb's and Lorentz's forces coupled with the geomagnetic field. Eddy current is not generated in the case of translation in the uniform magnetic field like free fall in geomagnetic field.

Coulomb's force in this case is interaction between the electrostatic charge on the falling object and the charges induced on the inside wall of the vacuum chamber by an electrostatic induction. The charge induced on the side wall of the vacuum chamber causes a horizontal force only, because the side wall is vertical and flat enough to generate this com-

ponent of the force only. It does not disturb the vertical motion of the falling object. The vertical force appears mainly at the time of the start and the end of the drop because of charges on the top plate of the inside frame and the bottom of the chamber. The interactions can be estimated under an assumption that the induced charges on the top plate, side wall and the bottom are proportional to solid angles subtended by respective parts from the center of the falling object. The inside dimension of the vacuum chamber is 394 mm in length and 107 mm in diameter. Supposing the falling object is a point charge, recording of its falling distance begins at the time when the falling object reaches a point about 7.5 mm below the top plate of the inside frame. The solid angle of the top plate at this moment is $0.43\times 4\pi$. Assuming that induced charge on the top plate is concentrated at its center, Coulomb's force in this case becomes $f=QQ'/4\pi\varepsilon_0 r^2=4.3\times 10^{-10}$ N, and the acceleration is $f/M=1.9$ μGal. The acceleration, due to this force, rapidly decreases as the falling distance increases. Variation in acceleration due to Coulomb's force, including the same effect of the bottom plate, versus the falling time is shown in Fig. 7-3. The mean effect does not exceed 0.3 μGal.

The motion of a charged falling object in a geomagnetic field is affected by Lorentz's force. The equation of motion in this case is

$$m\boldsymbol{a}=m\boldsymbol{g}+e(\boldsymbol{v}\times\boldsymbol{B}), \tag{7-45}$$

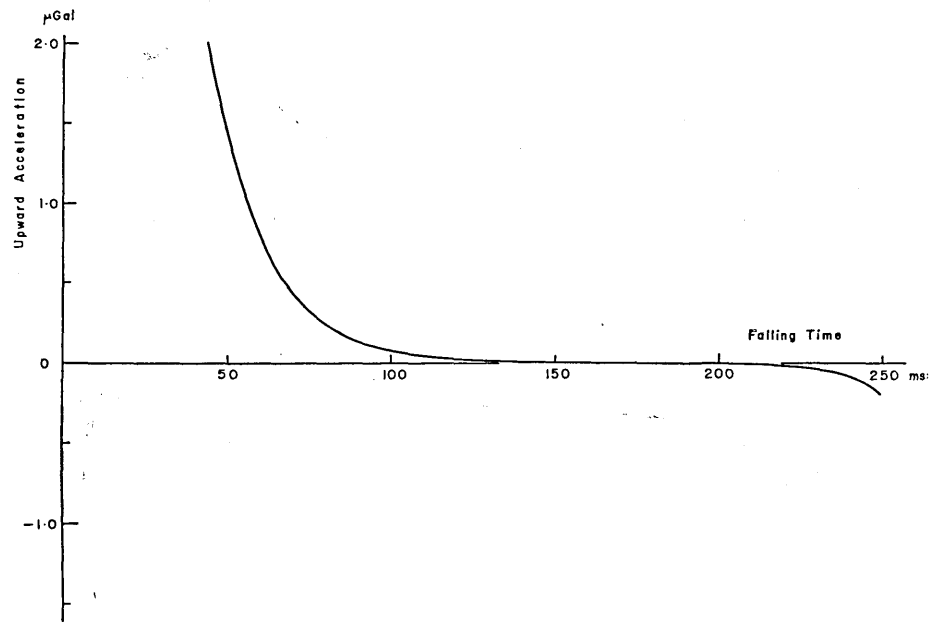

Fig. 7-3. Upward acceleration due to electrostatic charges induced on a falling object when contact potential is 1.0V.

where m is the mass of a falling object, $\boldsymbol{a}$, the acceleration, $\boldsymbol{g}$, the gravitational acceleration, $\boldsymbol{v}$, the velocity, and $\boldsymbol{B}$, the magnetic flux density of the geomagnetic field. Taking the z axis downward vertical, the solution of the equation under the initial conditions of $(x, y, z)=(0, 0, 0)$, $(v_x, v_y, v_z)=(0, 0, 0)$, $(a_x, a_y, a_z)=(0, 0, g)$ and $B=(B_x, 0, B_z)$ is

$$\left.\begin{aligned} x&=\frac{B_xB_z}{\omega^2B^2}g\left(\cos\omega t+\frac{1}{2}\omega^2t^2-1\right),\\ y&=\frac{B_x}{\omega^2B}g(-\sin\omega t+\omega t),\\ z&=\frac{B_x^2}{\omega^2B^2}g(-\cos\omega t+1)+\frac{1}{2}\frac{B_z^2}{B^2}gt^2, \end{aligned}\right\} \tag{7-46}$$

where $B=|\boldsymbol{B}|$, and $\omega=eB/m$. If we take $e=6.6\times10^{-12}$ C, $B_x=3.03\times10^{-3}$, and $B_z=3.42\times10^{-3}$ Wbm^{-2}, we have $\omega=1.3\times10^{-14}$ s^{-1}. From (7-46), we obtain

$$\frac{d^2z}{dt^2}=g-\frac{1}{2}\frac{B_x^2}{B^2}g\omega^2t^2. \tag{7-47}$$

Although (7-47) indicates that the downward acceleration decreases with the increase of falling time, its deviation from g is very small, such as $|(\ddot{z}-g)/g|<4\times10^{-30}$. Thus it can be said that the effect of geomagnetism is very small and it is unnecessary to take it into account.

7.9. Delay of Electric Signal in Electronic Circuits

Intensity variation of the interference fringe is converted into an electric signal by an avalanche photodiode and displayed on an oscilloscope. Though a constant delay occurring in this process is not effective, increase in falling velocity results in an increase in the frequency of interference fringes, i.e., that of the electric signal. Increase in the frequency of electric signals may be a source of systematic errors because of the phase characteristic of the electronic circuit which usually causes an increasing delay of the signal with its increasing frequency. Difficulty in measuring the variation of delay can be overcome by electronic circuit devices so constructed that the flat ranges of phase characteristic of employed circuits are wide enough and no appreciable delay change occurs within the signal frequency range.

It is necessary to estimate the required range of the phase characteristic. A phase shift at a frequency f relative to a low frequency range can be expressed as $-\mathrm{Arctan}(f/f_b)$, for a simple amplifier whose band width is f_b. To suppress a phase shift within a 0.01 phase angle $(=0.01\times2\pi)$ of a single cycle wave pattern with an accuracy of 0.01 mGal at a maximum signal frequency of 7.7 MHz, the necessary band width

f_b is estimated as at least 123 MHz. The electronic circuits used here have sufficiently wide ranges of phase characteristics, for example, the avalanche photodiode has 1 GHz range and the oscilloscope has 250 MHz range. Strictly speaking, as the oscilloscope used is widened in its frequency range by employing special technics such as emitter peaking treatment, its phase characteristics are not always simple nor flat. But it is in the higher frequency range that the effect of such a peaking treatment has to be taken into account, and it is believed that it is not a problem in such a low frequency range of 8 MHz.

7.10. Temperature

Temperature variation is usually one of the most serious disturbing factors in precise measurements. However, it has no effect in the present instrument, because we use a He-Ne laser as a length standard and a Rb frequency standard as a time standard. Both standards utilize transitions between energy levels of respective atoms. It is considered that effects of temperature change on the transitions do not exceed the aimed accuracy.

Other effects of temperature such as thermal expansions of the physical dimensions of each part of the instrument are also negligible because of a short measuring time.

7.11. Instrumental Oscillations

Although the motion of a falling object itself is not disturbed by instrumental oscillations, the interferometer is oscillated by them. This means that the measured distance contains the effects of external vibrations, whatever their sources may be. These effects, as expected, are one of the most serious disturbing factors.

Supposing a vertical oscillation of the instrument is expressed as $x=A\cos(\omega t+\phi)$, this is involved in the measured falling distance. When the measured falling distance is approximated by a quadratic function of time in the least-square approximation, the effect of oscillation can be determined by the following condition,

$$\int_0^T (x-at^2-b-c)^2 dt=\min. \tag{7-48}$$

That is,

$$a=\frac{60A}{T^2}\frac{1}{p}\cos\left(\frac{p}{2}+\phi\right)\left\{\frac{6}{p}\cos\frac{p}{2}+\left(1-\frac{12}{p^2}\right)\sin\frac{p}{2}\right\}, \tag{7-49}$$

where T is a total falling time and $p=\omega T$.

The effect on gravity Δg is obtained by $\Delta g=2a$. Fig. 7-4 shows this effect when we take $A=1\ \mu$m and $T=0.25$ s. The maximum effect

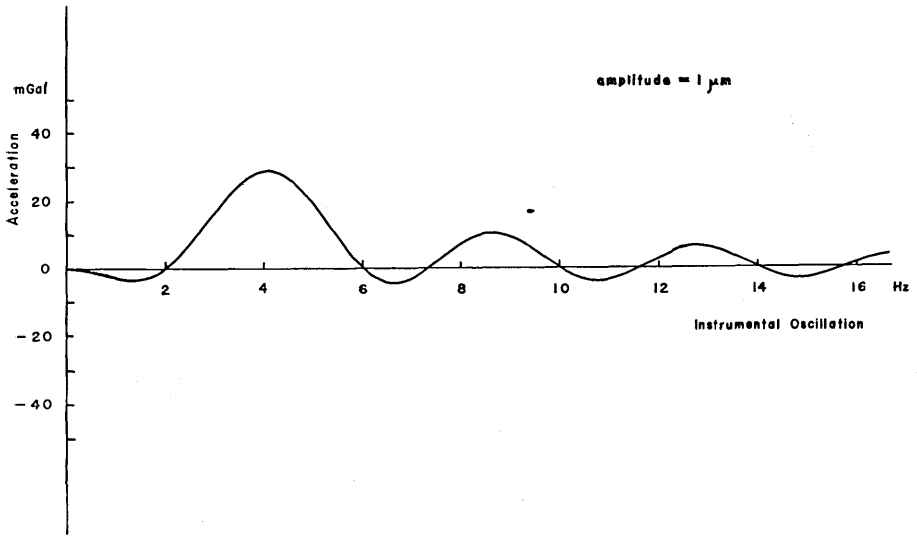

(a) A=1 μm, ϕ=0

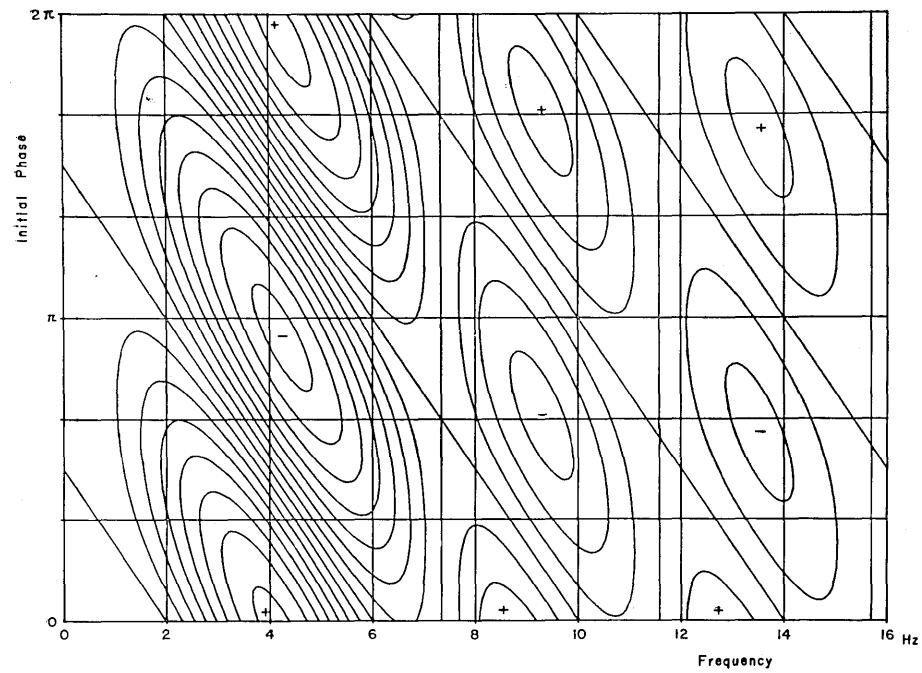

(b) A=1 μm. Contour intervals: 4 mGal. Straight lines represent zero mGal.

Fig. 7-4. Effect of the instrumental oscillation; $A\cos(\omega t+\phi)$.

appears at 4 Hz frequency in the case of $\phi=0$. The amplitude in acceleration of the instrumental oscillation is 63.2 mGal ($=\omega^2 A$) in this case. At the same time, it is found from (7-49), that the oscillation effect on the measured gravity reaches 29.2 mGal. This is about 46 percent of the disturbing acceleration. The reason why 4 Hz frequency gives the maximum effect is that this wave is well approximated by the quadratic function of time for $T=0.25$ s. When the frequency of the instrumental oscillation decreases toward 0 Hz, the ratio of the involved amplitude in the obtained gravity to the acceleration amplitude of oscillation increases until it reaches 100 percent at 0 Hz frequency. But its value itself decreases to 0 mGal because of the decrease in amplitude of the acceleration of the instrumental oscillation, since the acceleration amplitude is equal to $\omega^2 A$. It is interesting to note such an effect also decreases toward a higher frequency region in spite of a rapid increase of instrumental acceleration amplitude and it is due to the effective smoothing of the effect of the oscillation. It is one of merits of the continuous recording method employed in the present system.

The expected standard error of an obtained gravity value due to the instrumental oscillation, under the condition that the distribution of the initial phase ϕ is at random, is expressed as

$$s_g=\left|60\sqrt{2\pi}\,B\frac{1}{p^5}\left\{6p\cos\frac{p}{2}+(p^2-12)\sin\frac{p}{2}\right\}\right|, \qquad (7\text{-}50)$$

where B is the amplitude of acceleration of the instrumental oscillations. The maximum s_g appears when $p=2.127$, this corresponds to the frequency of 4.254 Hz at $T=0.25$ s. If we take $A=1$ μm, the amplitude of the acceleration of instrumental oscillations at this frequency amounts to 71.5 mGal. Its effect on the standard error of the result is about 36.9 mGal, about 52 percent of the overall effect of the instrumental oscillations.

8. Observation at Matsushiro

8.1. Preparation

The performance of the instrument used for the present study will be described in this chapter on the basis of data obtained in test observations. An experimental observation for its practical use was carried out at Matsushiro in Nagano Prefecture. Most of data was obtained at this experiment, but we also use other data, obtained at experiments carried out in the course of the developement of the instrument at the Kakioka Geophysical Research Observatory, Faculty of Science, the University of Tokyo. These experiments were carried out in October and

December 1974, and March and August 1975.

The following improvements have been made after the experiments at the Kakioka Geophysical Research Observatory.

1. The striking hammer was removed. The striking hammer had been prepared to give the supporting beam the initial motion in the early stage of the instrument's developement. This striking hammer was later removed because the instrumental vibrations excited by the shock of the starting hammer were so large that the amplitude of shock vibrations exceed one fringe (0.3 μm) in double amplitude. Such a large amplitude made it rather difficult to synthesize the fringe count from fringe patterns without mistake. It had once been believed that it was excited by collision between the hammer and the supporting beam, but the experiments made it clear that the cause of vibration was not a collision but the start of the hammer itself due to the principle of action and reaction. Therefore the hammer was replaced by the simpler present method, i.e., the push-spring method. As for the instrumental vibration, it will be mentioned in the forthcoming section.

2. A water supply for cooling system for the diffusion pump was changed from a drain system to a circulation system, because it is not always possible to utilize water supply according to conditions of the observation site.

3. Double speed sweep in the displaying fringe patterns on the oscilloscope.

4. Triggering of the drop by a vertical seismometer. As for these two items descriptions have been already made in Section 4.6.

8.2. Site and Period of Observation

An observation was made at the Seismological Observatory, Meteorological Agency in Matsushiro, in Nagano Prefecture. The observation site is located at the floor of the observation tunnel about 200 m distant from its entrance. The place is latitude 36° 32′ 31″ N, longitude 138° 12′ 25″ E, and elevation 407 m, as shown in Fig. 8-1.

A metal mark has been installed there for the convenience of reoccupation. Figs. 8-2 and 8-3 show the observation site and the metal mark. The period of observation was from July 15 to July 30, 1976.

8.3. General Situation of Observation

As it had been known in advance that amplitudes of ground vibrations decrease at night (YAMAGISHI, 1975), the observations were made mostly in the night time. Records were analyzed in a reverse order of the drop number taking the following fact into account, that the degree of vacuum became lower in later stages of experiment. Descriptions

about each drop were listed in Tables 8-1 and 8-2.

Two falling objects were used as denoted by Nos. 3 and 4 respectively in Table 8-1. The column of orientation in this table represents the azimuth which is faced by the specified portion labeled as '1' of the side wall of a falling object. The falling object was manually rotated 90° around its axis every time the recording film was refilled at intervals of seven or eight drops. The vacuum of the chamber had to be broken to make this rotation because no mechanism had been prepared in the instrument for this purpose. But such a rotation of a falling object is necessary, because that direction of inclination of a falling object must be statistically distributed

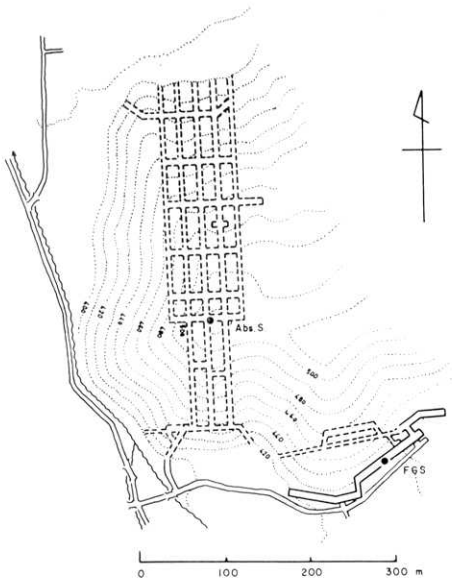

Fig. 8-1. Seismological Observatory.
Abs. S.: Site of the absolute measurement
FGS: First-order gravity station of the Geographical Survey Institute

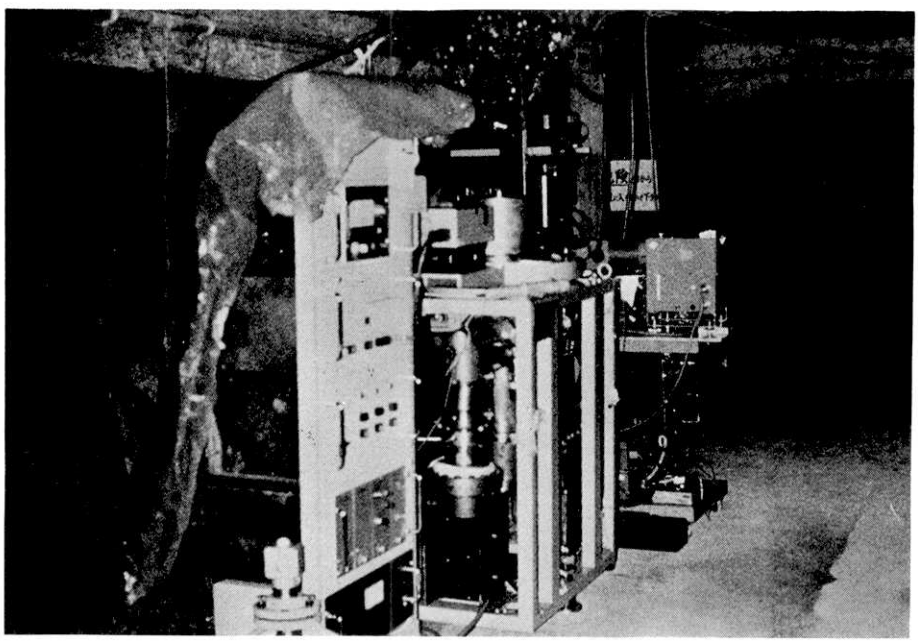

Fig. 8-2. Observation site.

uniformly around its axis. Change in the optical path length due to the inclination may be distributed at random through this process and the corresponding effects can be eliminated by taking the mean value of obtained data.

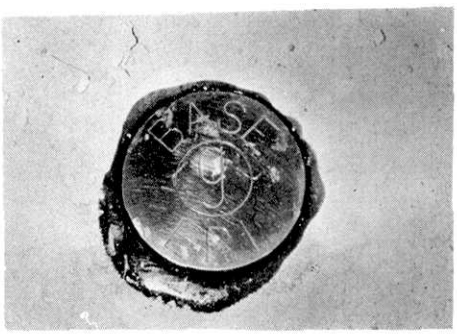

Fig. 8-3. Metal mark.

Operation of the laser used for a falling distance measurement became so unstable in the last period of observation that frequent interruption of the discharge in the laser tube occurred.

8.4. Results

Fig. 8-4 shows an example of the obtained film records of interference fringes. Bright fifty traces at the first parts of record are due to the slow sweep speed of 1 μs/div. Afterwards the speed is turned into 0.1 μs/div. Decrease in the interference fringe frequency at the end of the record indicates the fact that the vertical velocity of a falling object decreases at the collision against the stopper.

Appendix I gives an example of the distributions of amplitudes,

Table 8-1. Experimental data on recording film.

Film No.	Drop No.	Time of drop	Falling object	Orientation	Remarks
1	1- 8	17 July, 11^h, 12^h	3	N	
2	9- 17	16^h, 17^h	3	S	
3	18- 26	20^h, 21^h	3	S	
4	27- 34	22^h, 23^h	3	E	
5	35- 43	18 July, 17^h	3	W	
6	44- 51	20^h	3	W	
7	52- 60	20^h, 21^h	3	N	manual trigger
8	61- 69	19 July, 15^h, 16^h	4	N	
9	70- 77	19^h, 20^h	4	E	
10	78- 85	21^h, 22^h	4	S	
11	86- 94	20 July, 15^h, 16^h	4	W	
12	95-102	16^h	4	W	pressure experiment
13	103-109	27 July, 20^h	4	N	
14	110-117	22^h	4	E	
15	118-125	28 July, 14^h, 15^h	4	S	
16	126-133	16^h, 17^h	4	W	
17	134-141	22^h	3	N	
18	142-148	29 July, 07^h	3	S	

Table 8-2. Experimental data on each drop.

Drop No.	Data	Time (JST)	Lamb dip position*	Pressure
		h m	div	$\times 10^{-6}$ Torr
78	19 July	21 47	1245	15
79		21 52	1262	14
80		21 55	1268	14
81		22 00	1247	13
82		22 03	1274	13
83		22 06	1243	12
84		22 10	1243	11
85		22 13	1236	11
86	20 July	15 34	1404	13
87		15 38	1357	11
88		15 40	1346	12
89		15 43	1340	12
90		15 47	1340	12
91		15 51	1328	11
92		15 57	0092	11
93		16 00	1412	10.5
94		16 03	1350	10.5
95		16 16	1396	20
96		16 20	1392	20
97		16 24	1423	40
98		16 27	1365	60
99		16 31	1352	85
100		16 34	1302	100
101		16 40	1298	200
102		16 46	1306	400
103	27 July	20 01	1442	6.5
104		20 06	1434	6.5
105		20 10	1420	6.5
106		20 17	1422	6.5
107		20 19	1408	6
108		20 23	1442	6
109		20 26	1375	6
110		22 03	1268	8
111		22 07	1290	7.5
112		22 12	1256	7
113		22 17	1283	6.5
114		22 25	1235	6.5
115		22 34	1252	6
116		22 37	1255	6
117		22 45	1254	6

(to be continued)

Table 8-2. (Continued)

Drop No.	Date	Time (JST)	Lamb dip position*	Pressure
		h m	div	$\times 10^{-6}$ Torr
118	28 July	14 30	1118	6
119		14 35	1020	6
120		14 38	0820	6
121		14 45		
122		14 50	1432	5.5
123		14 54	0887	6
124		14 59	1170	5.5
125		15 03		6.5
126		16 47	1056	6.5
127		16 52	1054	7
128		16 57	1363	7
129		17 00	1185	6.5
130		17 07	1196	6.1
131		17 10	1448	6.5
132		17 14	1426	6.2
133		17 16	1112	6
134		22 22	1072	6
135		22 25	1118	6
136		22 28	1108	5.5
137		22 33	1071	6
138		22 38	1310	5.5
139		22 43	1094	5.5
140		22 47	1056	5.5
141		22 51	1085	5
142	29 July	07 16	1087	9.5
143		07 21	1083	8
144		07 29	1103	7.5
145		07 35	1070	8
146		07 41	1076	7
147		07 45	1118	7
148		07 49	1115	6.5

* Supplied voltage to the piezoelectric element expressed by dial division.

frequencies and initial phases of sine curves fitted to the respective interference fringes. An example of synthesized interference fringe wave counts is also found in Appendix II

Results obtained from No. 78 to No. 148 drops are shown in Table 8-3. The drops on and after the film numbered 15 were not used to obtain the final result, because although records were taken by utilizing intermittent radiations in the time of the unstable operation of the laser,

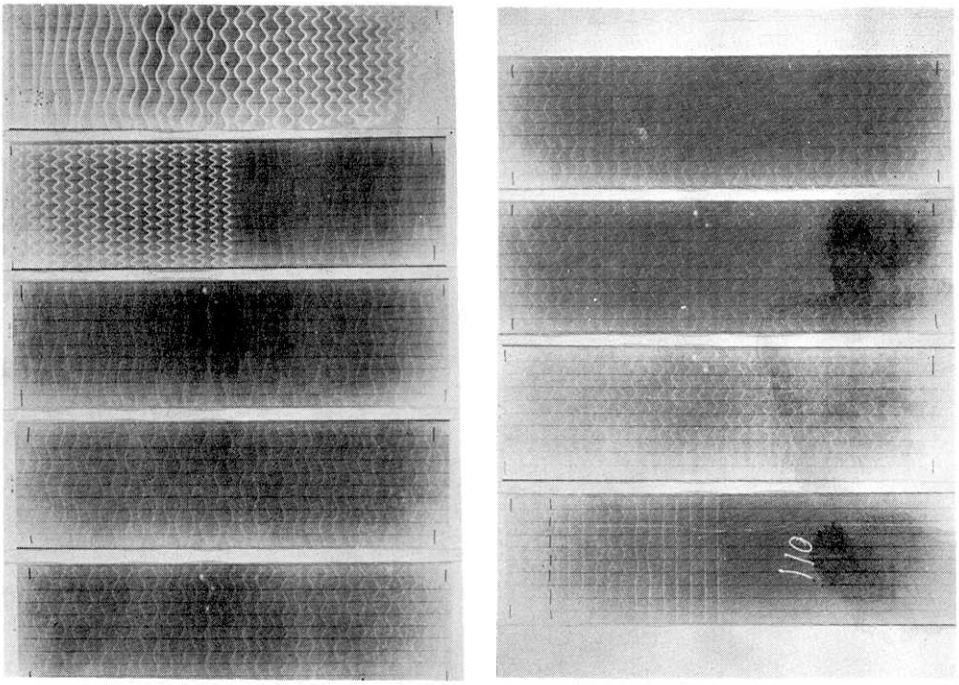

Fig. 8-4. A record of interference fringes (drop No. 110), Time sequence is from top to bottom and from left to right.

the results were scattered too much because of the poor setting of the wavelength of the laser into the Lamb dip, as shown in Fig. 8-5. The data on the right side of the dashed line in Fig. 8-5 was not used. Earth tide corrections were made on each result assuming the tidal factor to be 1.2. Inner gaseous pressures were distributed in a range of $6\sim14\times10^{-6}$ Torr, except during the time of the pressure experiment. This pressure range is an ultimate value at that time. Difference in pressure corresponds to a difference in the temperature of cooling water and evacuation time.

The obtained results without earth tide corrections, plotted against observation times, together with tidal variation curve seem to be consistent with the tidal variation as shown in Fig. 8-6. This tendency is shown more clearly in Fig. 8-7, in which the original results and the results after the earth tide correction are plotted. It is evident that the latter consistency is much better.

In Table 8-3, standard errors of the results were calculated by fitting a quadratic function of falling time to the corresponding series of synthesized fringe counts. It works as a indicator if the drop was normal. The fact that the results have standard errors of the same magnitudes

Table 8-3. Obtained results for each drop.

Drop No.	Gravity value		Error	Remarks
	Observed	After tidal correction		
	mGal	mGal	mGal	
78				no convergence
79	979 769.951	979 769.892	0.003	
80				no convergence
81				no convergence
82	940	880	003	
83				no convergence
84	968	907	003	
85				film end
86				camera slow start
87				irregular data
88	901	883	003	
89				irregular data
90	884	876	003	
91	966	949	003	
92				trace sweep miss
93				irregular data
94	855	838	002	
95-102				pressure experiment
103				no signal
104	928	869	003	
105	951	869	003	
106	958	880	003	
107	868	791	004	
108	915	838	004	
109	971	897	003	
110	879	860	003	
111				irregular data
112	885	869	003	
113	859	845	003	

and that most of them are not greater than 3 μGal implies that equal weights can be applied to each drop to take the mean value.

The mean value of sixteen drops from drop No. 79 to No. 113 is $g=979\ 769.870\pm0.036$ mGal. Drops from No. 96 to No. 101 were omitted in this calculation, since these experiments were made only to investigate the effect of residual gas. The gravity value at zero pressure was found to be:

$$g_0=979\ 769.892 \text{ mGal.}$$

Pressure correction is treated in the next section. The equivalent instrumental height was 0.76 m in this case. Using the mean vertical gradient of gravity, 0.3086 mGal/m, the correction of the instrumental height to the ground level becomes 0.235 mGal.

The result is shown as follows together with corrections,

gravity value at zero pressure		979 769.892 mGal
correction	instrumental height	0.235
	finite light velocity	0.004
result		979 770.131 mGal.

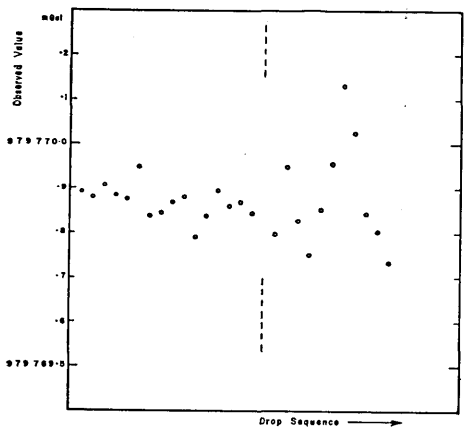

Fig. 8-5. Distribution of the results. The results in the latter part, right side of the dashed line in the figure, were not adopted.

8.5. Discussion

There are many disturbing factors affecting accuracy as studied in Chapter 7. We will treat experimental studies about the resettability of laser wavelength, the inclination of a falling object, pressure effect and microtremors in this section. We will also introduce residuals from a quadratic function of time fitting to falling distance.

8.5.1. Laser Wavelength

Accuracy of laser wavelength affects directly the accuracy of falling distance as mentioned before. Close investigation has revealed variations in wavelength due to its oscillation conditions (ENGELHARD, 1966; ENGELHARD et al., 1971), so that wavelength of respective lasers has to be calibrated. Another standard is necessary to calibrate a laser wave-

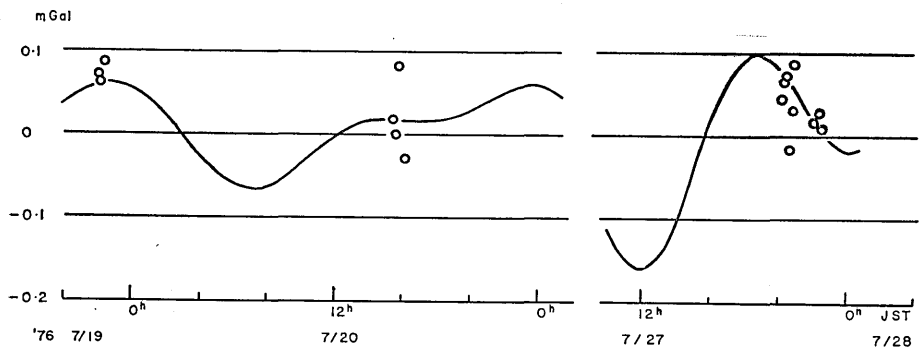

Fig. 8-6. Tidal curve with the obtained results.

length. This problem is now being requested in the National Research Laboratory of Metrology. The value of 632.99142 nm (MIELENZ et al., 1968) has been temporarily adopted as the laser wavelength which was used for the present work.

The resettability of laser wavelength also has to be investigated. The necessary limit of resettability has been already mentioned in Section 7.1. The experimental result is discussed here. Although an accurate investigation is impossible without a wavelength standard, the following simple method was adopted. Fig. 8-8 shows the rela-

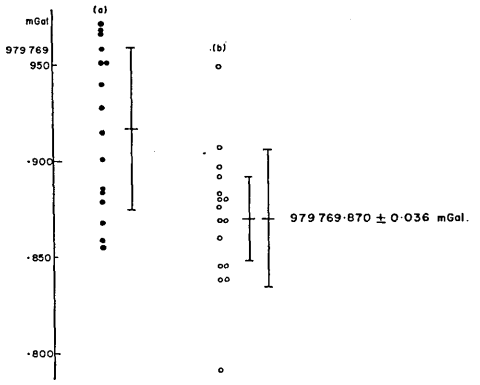

Fig. 8-7. Distribution of the results.
(a) Before tidal correction
(b) After tidal correction
Error bars represent standard errors for a single drop. Left side error bar in Fig. (b) corresponds in the case that maximum and minimum results are excluded.

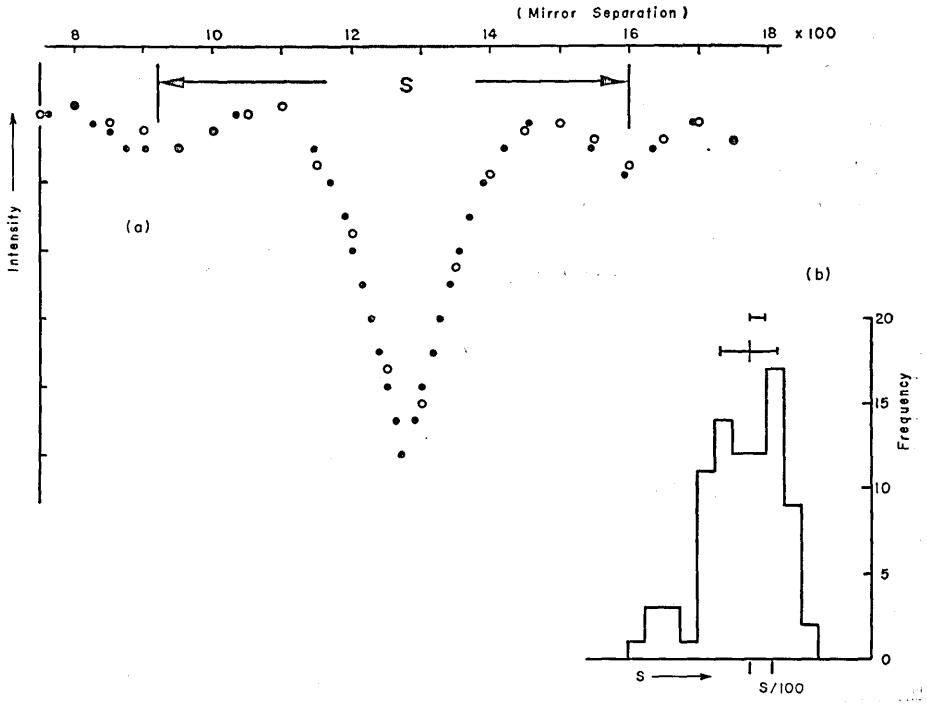

Fig. 8-8. Lamb dip (a) and its setting accuracy (b).
The error bar indicates the standard error for a single setting.
The short bar above the error bar shows the limiting accuracy for 0.01mGal.

tions between applied voltages to a piezo element which adjusts mirror separation and output light intensities. This relation was used for the experiment. The oscillation state is set into one of the two Lamb dips shown in the Figure. The resettability, the setting accuracy of the oscillation state to one of the Lamb dips, is repeatedly monitored with reference to the other Lamb dip. The mean length of s, the separation between two Lamb dips, is 694.5 with a standard error of 12.0 in a unit of division on the dial adjusting the piezo voltage. The setting accuracy of one margin of s is $\sigma=12.0/\sqrt{2}=8.5$, and the relative setting accuracy of the Lamb dip is found to be $\sigma/s=1.22\times10^{-2}$. It has been found in Section 7.1. that the setting accuracy of the wavelength should be restricted within 6.25×10^{-3} in mirror separation to ensure the accuracy of the observed gravity within 0.01 mGal. The obtained result on the wavelength has an error twice as great as that necessary for 0.01 mGal gravimetry. The relations among respective values are found in Fig. 8-8.

It has been found from our experiments that the obtained gravity value has a standard error of ±0.020 mGal due to the inaccuracy of the setting of the laser wavelength. The observational error of 0.036 mGal obtained in Section 8.4. contains such an error due to the wavelength setting, that is to say, the error of wavelength setting and those due to other sources are estimated as 0.020 and 0.030 mGals, respectively, so that the overall error amounts to 0.036 mGal.

8.5.2. Inclination of a Falling Object

Variation in optical path length due to the inclination of a falling object has been discussed in Section 7.7. We will describe here the actual inclinations of a falling object and an estimation of its effect on obtained gravity value.

Experiment on Inclination of a Falling Object

As a cat's eye does not show its inclination explicitly because of the parallelism of the incident with reflected rays, a dummy glass cylinder with the same outside dimension and which has a plane reflection surface at its head is used instead of a falling object. The inclination of this dummy is recorded by the following method. A falling dummy is illuminated by a collimated strobolight flashing with intervals of 20 ms. Reflected rays by the dummy are brought to a spot on a photographic film through a collimator. Thus the inclination of the falling dummy can be recorded. A systematic tendency of inclination is evident in Fig. 8-9. Some samples of reflected images are shown in Fig. 8-10. (a) is a case where inclination is comparatively large. A large central spot is formed by multiple lights from the dummy in a fixed position before its drop. A chain of thirteen spots is made by light reflected from the falling

dummy which inclined 11.5′ during its fall. Spots after the stop of the dummy vanish because of its large inclination. Another example, (b), shows a case of small rotation. The total angle of inclination is only 2′. Thirteen dots of flashed light seem to be a segment of a line instead of a chain. The theoretical limit of inclination has been found to be 3.5′ in Section 7.7. The smaller value of 2′ may mean an action of some other moment by an irregular initial motion which cancels the effect of gravity. The exertion of some moment other than gravity is also suspected from a discrepancy between the direction of inclination and that of the motion of the supporting beam. It may be presumed as a cat's eye has also the same order of inclination.

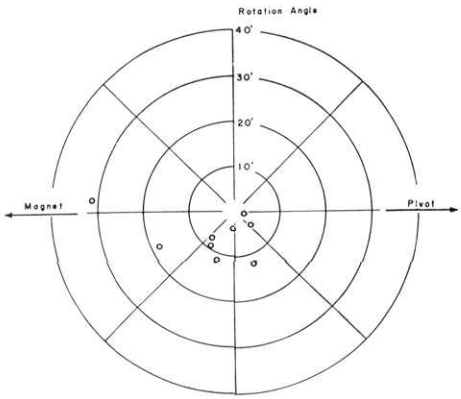

Fig. 8-9. Distribution of inclinations of a falling mirror.

Effect of Inclination on Measured Gravity Value

Table 8-4 shows classified results with respect to the orientations of a falling object. It generally seems that southward and westward orientations gained large results as compared with the other orientations. The effect of inclination on measured gravity values is expressed as

$$g=979\ 769\ 872.75+24.7 \sin(\theta+216^\circ)\ \mu\text{Gal}, \tag{8-1}$$

where θ is the angle reckoned anticlockwise from the east. Deviation of gravity value at each azimuth does not exceed 0.25 μGal from the plane distribution. It may be considered that the obtained result shows the existence of systematic variations in an optical path length with the

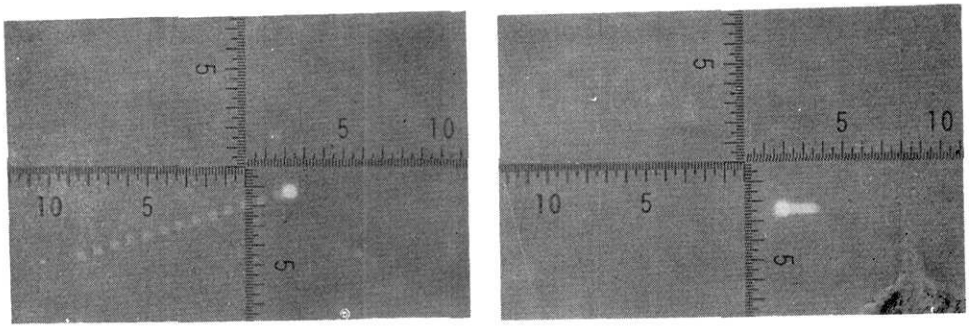

(a) (b)

Fig. 8-10. Examples of records of inclination of a falling mirror.

Table 8-4. Classified result according to orientations of a falling object.

Orientation	Gravity value	Std. error
	mGal	mGal
S	979 769.893	0.014
W	887	0.046
N	853	0.046
E	858	0.012

Table 8-5. Analysis of variance for the gravity orientation relation.

	Data				
	S	W	N	E	
	979 769.892	883	845	860	
	880	876	869	869	
	907	949	880	845	
		838	791		
			838		
			897		
Sum	2679	3546	5120	2574	13919
N	3	4	6	3	16
Mean	893.0	886.5	853.3	858.0	869.9

Factor	Square sum	Degree of freedom	Unbiased variance	Variance ratio
Between class	4774.61	3	1591.54	F=1.355
Within class	14094.33	12	1174.53	
Total	18868.94	15		

$F_{3,12;0.01}=5.95$

$F<F_{3,12;0.01}$

direction of the inclinations of a falling object. However, gravity values at respective azimuths have rather large variances, and the analysis of variance reveals the insignificance of interclass variance on the azimuth-gravity relation. (Table 8-5) Consequently, the differences of gravity values due to the orientation of a falling object can be neglected and the simple mean of all the gravity data can be adopted as results.

8.5.3. Effect of Residual Gas

As an obtained gravity value is strongly affected by residual gas in

Table 8-6. Pressure—gravity relationship.

Drop No.	Pressure	Gravity	Weight
	$\times 10^{-6}$ Torr	mGal	
	9	979 769.870	16*
96	20	927	1
97	40	760	1
98	60	767	1
99	85	692	1
101	200	463	1

* Mean value of the results at ultimate pressures.

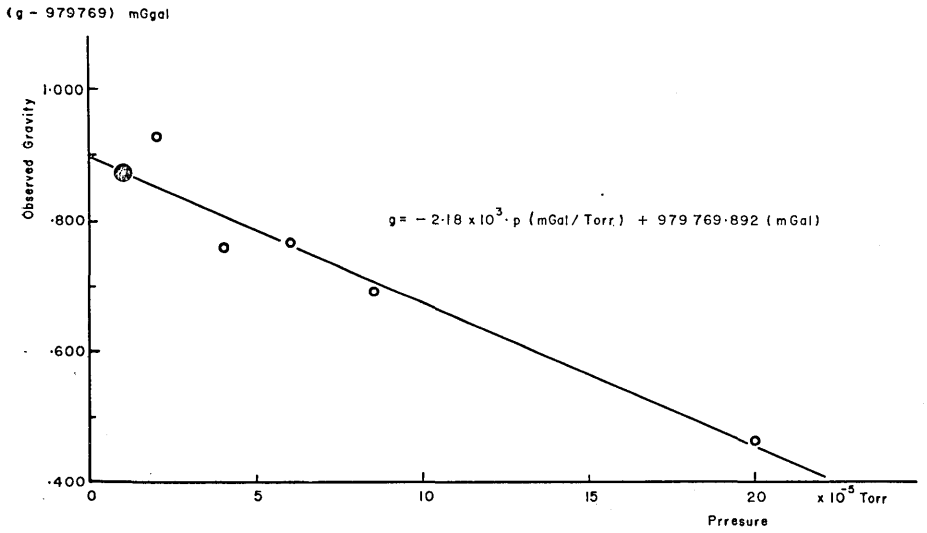

Fig. 8-11. Pressure—gravity relation.

a simple free fall as compared with a symmetrical free fall, it is necessary to approach the effect experimentally as well as theoretically. Drops No. 95～No. 102 were carried out for this purpose. The range of pressure was from 2 to 40×10^{-5} Torr. Pressures and measured gravity values are listed in Table 8-6. The result of an ordinary measurement in an ultimate pressure is also included in the list. The relation between pressure and gravity is also illustrated in Fig. 8-11. Their linear relation has been confirmed by theoretical consideration in Section 7.5. The relation fitted by the least-square approximation is expressed as

$$g=(-2.18\pm0.11)\times p\times10^{3}\,\mathrm{mGal/Torr}+979\ 769.892\pm0.005\,\mathrm{mGal}.$$

The theoretical value of the pressure coefficient has been found to be

1.40×10^{3} mGal/Torr. (Section 7.5.) The obtained experimental value, however, is 1.56 times as large as the theoretical value. The difference may be caused by the theoretical assumption that a falling object has a smooth cylindrical surface, but 94 percent of the actual surface of a falling object is rugged and the effective surface area must be greater than the surface assumed as smooth. Such an order of discrepancy between the theoretical and experimental results can be explained by the difference in the surface area between the actual falling object, having a rugged surface, and the theoretical one having a smooth surface.

The mean inner pressure was $(9\pm2.8)\times10^{-6}$ Torr in the regular measurement. The ionization gauge used for this work has a poor accuracy of 20 percent of the full scale of the order to which the measured pressure value belongs in the indicator. Taking such uncertainties into consideration, the effect of residual gas on the accuracy of measurement is estimated to be $\pm8\times10^{-3}$ mGal.

8.5.4. Effect of Instrumental Oscillation

The period of the instrumental oscillations which affect the result lies, for the most part, in the range of two or three tenths of second as is shown in Section 7.11. This kind of wave is thought to come from ground microtremors rather than from instrumental origins. A research on microtremors at Matsushiro has been already carried out although mainly for the horizontal component (YAMAGISHI, 1975). According to this research, the range of the period which has a larger amplitude is from 0.2 to 0.6 seconds and the wave of a 0.4 second period has the maximum amplitude. The amplitude decreases in order of S-N, E-W, and U-D components. The amplitude of the S-N component is about 2 μkine during the night. If its period is 0.25 seconds, the acceleration amplitude becomes 50×10^{-3} mGal. Although we have no information about the U-D component, it may be allowable to estimate that the U-D component has a magnitude of the same order as that of S-N component. Thus, the microtremors having the amplitude of 50×10^{-3} mGal, give an effect of 0.026 $(=0.05\times0.52)$ mGal as a standard error to the measured gravity according to the discussion in Section 7.11.

Combining the errors mentioned above, all together, the obtained standard error of measured gravity is resolved as given in the following table.

microtremors	0.026 mGal
wavelength	0.020
pressure	0.008
vertical gradient of gravity	0.008
deviation from vertical of ray	0.002

other sources	0.015
overall	0.038 mGal

8.5.5. Residual

One of distinguishing features of the present instrument is that it is able to measure the falling distance every 1 ms almost continuously, so that the details of motion of a falling object can be detected even if an irregular variation is contained in falling distance. Another type of absolute instrument in which the minimum points have been prepared to detect the positions of a falling object may have some difficulty in removing an irregular variation in the falling distance. The continuous recording of falling distance overcomes such difficulties much more easily in the present instrument. To smooth the irregularity, we use a suitable function fitting the series data of the falling distance, such as a quadratic function of time, by which an effect of the vertical gradient of gravity is corrected afterwards. There is another way to correct the effect of the vertical gradient of gravity, in which the calculation is carried out by fitting directly a hyperbolic cosine function of time. Irregular variation can be kept out of the falling distance by these methods so long as they do not have a time square component, which has essentially the same form as gravity effect and can not be separated from each other. The residuals thus obtained can represent irregular vertical movements deviating from the pure free fall.

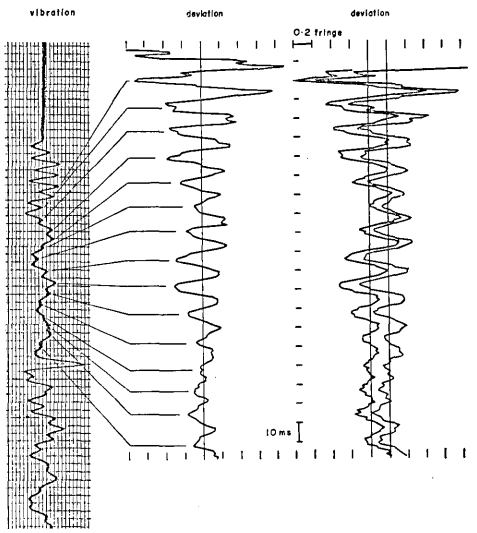

Fig. 8-12. Residuals of falling distances from the time squared function obtained at Kakioka (large amplitude case).
left: Record of a seismometer
middle and right: Three examples of residuals

Fig. 8-12 shows three examples of the distribution of deviation according to the falling time, which were obtained in the experiment at Kakioka. The upper part of this figure corresponds to the beginning of a drop and lower part to the bottom of a drop. It is noticed at a glance that every pattern of deviation contains oscillations whose mean period is about 13.6 ms with the same phase relations. The oscillations have large amplitudes at the beginning of drop and they decrease rapidly

with falling time. Therefore it has been estimated that the distribution of deviation represents instrumental vibration, oscillation of the interferometer, excited at the start of a falling object. Then a vertical motion seismometer whose period is about 0.9 s, was attached temporarily to the instrument for monitoring the instrumental vibration. A record of the seismometer is also seen on the left side of the same figure. The seismometer gives outputs proportional to velocity, while the deviation does not show velocity but displacement, so that direct comparison with both the records is not always appropriate. However, it is evident that the deviation is derived from the instrumental oscillation, judging from a good correspondence between both the wave patterns.

These records were obtained in the process of development of the instrument. The supporting beam was started by the shock of a driving hammer at that time. Hence the instrumental oscillation was considerably large and the amplitude of deviation reached almost one fringe at the early stage of the drop. As the present instrument observes only fractions of interference fringes, such a large deviation as exceeding one fringe may cause a mistake in synthesizing fringe count. Correction of such a mistake is, of course, possible and it is an advantage of the continuous recording system of the falling distance. The examples shown in Fig. 8-12 were made through this correction process. But it is needless to say that the smaller the amplitude of instrumental oscillation, the smaller its effect on the measured gravity. The triggering hammer has been therefore replaced by a pressure spring.

The reason for the lack of a record corresponding to the leading part of the seismogram is that there is some start-time difference between the instrumental oscillations and the drop of a falling object due to the hammer motion and that about 50 ms of falling time is necessary for a falling object to gain a sufficient velocity to display a sine-wave pattern of interference fringe. A large spike at the lower middle part of the seismogram indicates the collision of the falling object with the stopper. The seismogram also shows a slower wave, the period of which is about 60 ms, overlapping the instrumental oscillation. But there is no wave corresponding to this period clearly in the deviation of the falling distance. If the instrument actually oscillates with such frequencies, the residual of the falling distance shows such waves. So, it may be concluded that the wave of the 60 ms period is due to the frequency characteristics of the seismometer used and not an actual wave such as the instrumental vibration. The present instrument has a function as an absolute displacement monitor, in other words, the instrument realizes an absolute reference point which is completely free from outer disturbances through a free fall. This means in a sense that a quite new technique

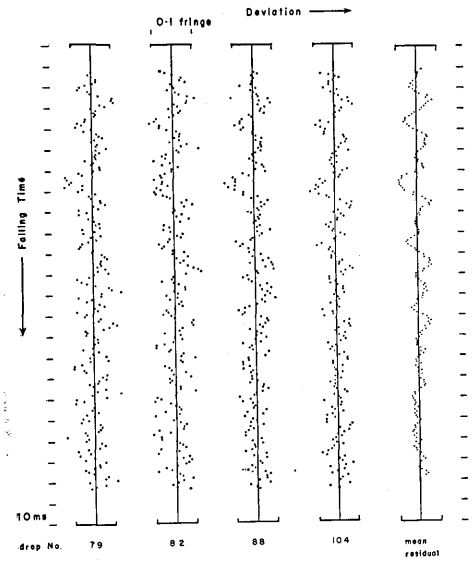

Fig. 8-13. Residuals of falling distances from the time squared function obtained at Matsushiro (normal case).

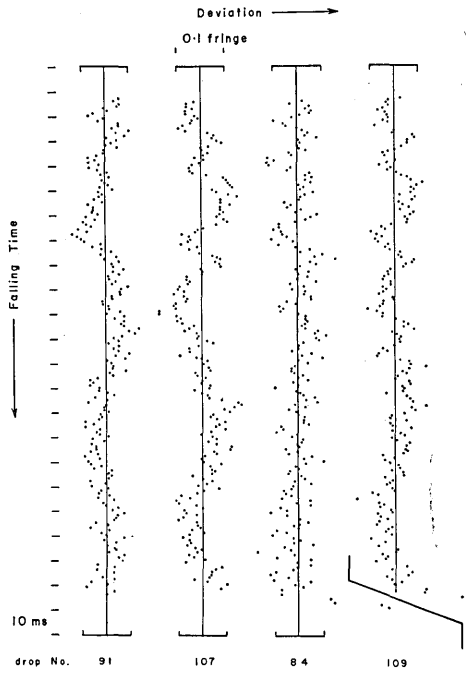

Fig. 8-14. Residuals of falling distances from the time squared function obtained at Matsushiro (abnormal case).

is offered in the field of seismometry by the present instrument.

Figs. 8-13 and 8-14 are examples of deviations obtained by the observation at Matsushiro. The amplitude of oscillation of the instrument is greatly reduced and does not exceed 0.1 fringe in double amplitude after the replacement of the starting device by a push spring. Oscillation disappears in the fluctuation of the record in the lower part of the drop in which its amplitude decreases. A typical pattern of oscillation is also illustrated in the Fig. 8-13. This pattern was obtained by taking an average of the deviations of corresponding traces of all drops. It seems that the instrumental vibration still remains.

From a viewpoint of gravity measurement, more interesting are the examples shown in Fig. 8-14 in which some abnornal deviations have been detected. Two examples (drop Nos. 91 and 107) contain slow oscillations whose periods are both about 90 ms overlapping ordinary instrumental vibrations. This means that some ground vibrations can be eliminated as residuals of falling distances, although the components of vibrations which can be expressed by a quadratic function of time are inevitably mixed into the results and disturb the obtained gravity value. It is

reasonable that, when a residual increases, the t^2 component also increases. In fact, the gravity values obtained from drops Nos. 91 and 107 are far apart from the average value. (Table 8-3) It is interesting to notice that the distributions of deviations seem to be in anti-phase for both drops with each other, and drop No. 91 has a too large result and No. 107 too small.

Other examples (drop Nos. 84 and 109) in the figure are the cases of rapid increase in residuals at the end of the drop. As a falling object stops finally, it must be decelerate near the end of the drop. These examples show accelerations unexpectedly greater than the normal free fall. This paradoxical phenomenon can be explained as follows. The stopper which receives a falling object is made of Teflon and shaped like a cylindrical cup. As a falling object slips into this cup at the drop end, frictional electricity is generated on both the falling object and the stopper. Static charges on the falling object are discharged through the electric conductivity of its surface and the vacuum chamber by a preparation process for next drop. Static charges on the stopper, however, remain through the whole period of measurement. When the falling object approaches to the stopper, the non-uniform distribution of charges appear on its surface by electrostatic induction. Acceleration of the falling object increases according to Coulomb's force exerted between these bodies. This is a mere presumption of the phenomenon at present but it may be supported by the increasing tendency of the phenomenon with the advance of the drop number and by the fact that this phenomenon disappears at the renewal of a recording film when the discharge of the electrostatic charges on the stopper would occur through manual handling of the inside of the vacuum chamber. This phenomenon has of course a bad effect on the result. But, there is no way to discharge the stopper without breaking the vacuum at present. Consequently, the last four traces of the interference fringe displays of each drop, which might be affected by Coulomb's force, are omitted.

The ability of investigating the detailed motion of a falling object as described above is an advantage of the continuous recording system of the falling distance which has been employed in the present instrument.

9. Comparison with Other Measurements

The First-order Gravity Station of the Geographical Survey Institute (FGS) is situated at the Seismological Observatory, Meteorological Agency, Matsushiro as represented in Fig. 8-1. Relative measurements have been made there several times on the basis of the Tokyo base station belonging to the Geographical Survey Institute, so that the comparison between

the gravity value of FGS and that of the absolute station obtained here, is possible.

The gravity value at FGS has been determined from eight observations as one of the stations in the Japan Gravity Standardization Net 1975 (JGSN 1975). The gravity value adopted is:

$$g=979\ 769.76\pm0.01\ \text{mGal}\quad\text{(Geographical Survey Institute, 1976).}$$

The above error represents the standard error of the result which has been obtained by relative measurement. In other words, it represents the accuracy of relative measurement. 0.1 mGal is more reasonable than 0.01 mGal as the standard error of the gravity value for the absolute value (SUZUKI, 1976), because 0.1 mGal is the order of the standard error of the International Gravity Standardization Net 1971.

The gravity difference between FGS and the absolute station has been found to be:

$$g_{\text{ABS}}-g_{\text{FGS}}=0.434\pm0.003\ \text{mGal}$$

by the LaCoste-Romberg gravity meter observation carried out at the same time with the absolute measurement observation. Then, the gravity value at the absolute station refered to JGSN 1975 is:

$$g_{\text{ABS}}=979\ 770.19\pm0.1\ \text{mGal.}$$

The result of the observation with the present instrument, combining the measured value with estimation of errors, is:

$$g_{\text{OBS}}=979\ 770.131\pm0.038\ \text{mGal.}$$

The difference between g_{ABS} and g_{OBS} is not greater than the standard error of g_{ABS}. This result may support the reliability of the observation by the present instrument and the value of JGSN 1975.

The standard error of 0.038 mGal of the present observation is that of a single measurement. The standard error of the mean value becomes $0.038/\sqrt{16}=0.010$ mGal. Thus it can be concluded that the present instrument has a measuring accuracy of the same order of relative measurement.

10. Conclusion

(1) A transportable apparatus for the absolute measurement of gravity has been successfully constructed in the Earthquake Research Institute. The principle of measurement of the apparatus is to utilize a simple free fall in which the falling distance is measured by optical interferometry using a manually controlled Lamb dip stabilized He-Ne

laser. A cat's eye with a length of 33 mm and a diameter of 20 mm is adopted as a falling object in order to make the instrument small. The falling distance is taken to be 30 cm and it is measured at every 1 ms interval in a single drop. The recording system is simply taking a photograph of the interference fringes displayed on an oscilloscope at the accurate constant rate of 1 ms. Only the phase angles of interference fringes are read on the photograph. The series of the increasing falling distance in a single drop is synthesized by utilizing the fact that the second difference of the series of falling distance is constant. This measuring system of falling distance is very useful for both simplifying the recording system and eliminating the effect of disturbing vibrations of the instrument.

(2) A test observation was carried out at the Matsushiro Seismological Observatory. The result obtained from sixteen drops was:

$$g = 979\ 770.131 \pm 0.038 \text{ mGal.}$$

A gravimetric connection between the present station and Matsushiro First-order Gravity Station shows that the present result is slightly smaller than the gravity value referred to JGSN 1975 system by 0.06 mGal. This discrepancy, however, is smaller than the estimated error of the value of FGS (0.1 mGal). The measuring accuracy of the present instrument is found to have about 0.04 mGal as the standard error of a single measurement and the practicability of the present instrument is confirmed.

(3) Among the disturbing factors which cause the scattering of observed value, the resettability of the wavelength of laser light, the vertical gradient of gravity, residual gas, microtremors are predominant. It is estimated that the standard error of 0.04 mGal of a single measurement is resolved into 0.026 mGal by microtremors, 0.020 mGal by resettability of laser wavelength, 0.008 mGal by uncertainty of the coefficient of vertical gradient of gravity, 0.008 mGal by inaccurate pressure measurement, and the rest by minor factors.

(4) As for the systematic error on the obtained gravity value, the wavelength of the laser is probably the most serious for the present state of the instrument. Its calibration is not possible because the length standard such as the ^{86}Kr primary standard is not available. But the improvement of the method of stabilization of the wavelength of the laser such as iodine saturated absorption will easily overcome this uncertainty. The systematic disturbances other than wavelength uncertainty due to factors such as the vertical gradient of gravity or residual gas are able to be eliminated by theoretical or experimental treatments until their residual effects become lower than a level of micro-Gal.

(5) The present instrument is the first one in Japan as a transportable apparatus for the absolute measurement of gravity with the highest measuring accuracy. The success of the development of the instrument is mainly due to the adoption of the continuous recording system of falling distance utilizing a laser beam. The instrument will be improved still more to have a higher measuring accuracy of a micro-Gal order by introducing an iodine saturated absorption stabilized laser and by adopting a more sophisticated measuring system such as rapid release of a falling object and triggering of the drop by microtremor phase detection.

Acknowledgments

The construction of the present instrument was originated under the leadership of Dr. Ietsune TSUBOKAWA, Director of the International Latitude Observatory of Mizusawa. The author's most sincere thanks are due to him for his constant guidance in the course of the work. The author is much indebted to Associate Professor Yukio HAGIWARA for his interest and encouragement, and also owes electronic circuits of the instrument to Mr. Michio YANAGISAWA. Frequent discussions with Dr. Ko NAGASAWA has stimulated the author. The author wishes to thank Professor Naoshi FUKUSHIMA, Director of the Geophysics Research Laboratory, the University of Tokyo and Dr. Mitsuo EDA, Director of the Seismological Observatory, the Meteorological Agency, for all their help in providing spaces for making experiments possible for this work.

References

1) AGALETSKY, P. N., K. N. YEGOROV and A. I. MARTSINYAK, 1959, Results of absolute determinations of the acceleration due to gravity by three independent methods in the point of the 'VNIM' (Leningrad). *Bull. Géod.* **51**, 82-90.
2) BARNES, D. F., 1966, Gravity change during the Alaska Earthquake. *J. Geophys. Res.* **71**, 451-456.
3) BARTA, G., 1971, On the hypothesis of the secular variation of gravity field. *Bull. Géod.* **100**, 165-173.
4) BELL, G. A., D. L. H. GIBBINGS and J. B. PATTERSON, 1973, An absolute determination of the gravitational acceleration at Sydney, Australia. *Metrologia* **9**, 47-61.
5) BESSEL, F. W., 1850, Construction eines symmetrisch geformten Pendels mit reciproken Axen. *Astron. Nachr.* **30**, 697, 1-6.
6) BOULANGER, J. D. and S. N. SCHEGOLOV, 1971, On secular changes of gravity. *Bull. Géod.* **100**, 175-178.
7) BOULANGER, J. D., 1973, Secular variations in gravity. *Proc. Symposium on Earth's Gravitational Field and Secular Variation in Position*. 205-212.
8) CLARK, J. S., 1939, An absolute determination of the acceleration due to gravity. *Phil. Trans. Roy. Soc. London, Ser.* A, **238**, 65-123.
9) COOK, A. H., 1957, Recent developments in the absolute measurement of gravity. *Bull. Géod.* **44**, 34-59.

10) COOK, A. H., 1965, The absolute determination of the acceleration due to gravity. *Metrologia*, **1**, 84-114.
11) COOK, A. H., 1967, A new absolute determination of the acceleration due to gravity at the National Physical Laboratory, England. *Phil. Trans. Roy. Soc. London. Ser. A*, **261**, 211-252.
12) CURTIS, A. R., 1951, Elasticity corrections for pendulums used in the absolute measurement of gravity. *Mon. Not. Roy. Astron. Soc. Geophys. Suppl.* **6**, 159-162.
13) DRYDEN, H. L., 1942, A reexamination of the Potsdam absolute determination of gravity. *J. Res. Nat. Bur. Stand.* **29**, 303-314.
14) ENGELHARD, E., 1966, Wellenlängenstabilität eines Neon-Helium-Lasers. *Z. angew. Phys.* **20**, 404-407.
15) ENGELHARD, E. and K. ABDEL-HADY MOHAMED, 1971, Pressure-wavelength relationship of the 6328-Å Helium-Neon laser emmision. *J. Opt. Soc. Amer.* **61**, 216-217.
16) FALLER, J. E., 1965, Results of an absolute determination of the acceleration of gravity. *J. Geophys. Res.* **70**, 4035-4038.
17) FALLER, J. E., 1965, An absolute interferometric determination of the acceleration of gravity. *Bull. Géod.* **77**, 203-204.
18) FALLER, J. E., 1967, Precision measurement of the acceleration of gravity. *Science* **158**, 60-67.
19) FRENKEL, J., 1924, Theorie der Adsorption und verwandten Erscheinungen. *Z. Physik* **26** 117-138.
20) THE GEOGRAPHICAL SURVEY INSTITUTE, 1976, Establishment of the Japan Gravity Standardization Net 1975. *J. Geod. Soc. Japan* **22**, 65-76.
21) GUILLET, M. A., 1938, Mesure precise de l'acceleration g de la chute des corps dans le vide. *Comptes Rendus Acad. Sci., Paris* **207**, 614-616.
22) HAMMOND, J. A. and J. E. FALLER, 1971, Results of absolute gravity determinations at a number of different sites. *J. Geophys. Res.* **76**, 7850-7854.
23) HEYL, P. R. and G. S. COOK, 1936, The value of gravity at Washington. *J. Res. Nat. Bur. Stand.* **17**, 806-839.
24) HONKASALO, T., 1970, Letter to Special Study Group 4.21 of the I.A.G. *J. Geod. Soc. Japan* **16**, 89-90.
25) HURLBUT, F. C., 1957, Studies of molecular scattering at the solid surface. *J. Appl. Phys.* **28**, 844-850.
26) INABA, F. and K. SHIMODA, 1973, Measuring technique on lasers. Laser Handbook. *Asakura Shoten, Tokyo*, 795 pp. (in Japanese).
27) JEFFREYS, H., 1949, The figures of the earth and moon. *Mon. Not. Roy. Astron. Soc., Geophys. Suppl.* **5**, 219-247.
28) KÜHNEN, F. and Ph. FURTWÄNGLER, 1906, Bestimung der absoluten Grossee der Schwerkraft zu Potsdam mit Reversionspendeln. *Veröff. Kgl. Preuss. Geodät. Inst.* N. F. **27**, 390 pp. (cited from Cook (1965).)
29) LAMB, W. E. Jr., 1964, Theory of an optical maser. *Phys. Rev.* **134**, A1429-A1450.
30) LAMBERT, A. and C. BEAUMONT, 1977, Nano variations in gravity due to seasonal groundwater movements: implications for the gravitational detection of tectonic movements. *J. Geophys. Res.* **82**, 297-306.
31) MIELENZ, K. D., K. F. NEFFLEN, W. R. C. ROWLEY, D. C. WILSON and E. ENGELHARD, 1968, Reproducibility of helium-neon laser wavelength at 633 nm. *Appl. Optics*, **7**, 289-292.
32) MORELLI, C., C. GANTER, T. HONKASALO, R. K. MCCONNELL, J. G. TANNER, B. SZABO, U. UOTILA and C. T. WHALEN, 1974, The international gravity standardization net 1971. Special publication No. 4, The international association of geodesy, 194 pp.
33) MOROKUMA, T., 1962, Interference comparator for routine measurement of length (I). *Oyo Buturi* (A monthly publication of the Japan society of applied physics), **31**, 192-

200. (in Japanese).
34) MURATA, I., 1970, On precise gravity survey in Miura and Boso peninsulas—some comments on the survey—. *J. Geod. Soc. Japan*, **16**, 44-53. (in Japanese).
35) PRESTON-THOMAS, H., L. G. TURNBULL, E. GREEN, T. M. DAUPHINEE and S. N. KALRA, 1960, An absolute measurement of the acceleration due to gravity at Ottawa. *Can. J. Phys.* **38**, 824-852.
36) SAKUMA, A., 1959, Absolute determination of gravity value by falling body methods. *Keisoku* (Journal of the Society of instrument technology), **9**, 511-523. (in Japanese).
37) SAKUMA, A., 1963, État actuel de la nouvelle détermination absolue de la pesanteur au Bureau international des poids et mesures. *Bull. Géod.* **69**, 249-260.
38) SAKUMA, A., 1971, Observations experimentales de la constance de la pesanteur au Bureau international des poids et mesures Sèvres, France.—Methode utilisee avec l'appareil de mesure absolue du B.I.P.M. et resultats sur 3 ans d'observations. *Bull. Géod.* **100**, 159-163.
39) SAKUMA, A., 1973, A permanent station for the absolute determination of gravity approaching one micro-gal accuracy. *Proc. Symposium on Earth's Gravitational Field and Secular Variation in Position*, 674-684.
40) SCHÜLER, R., G. HARNISCH, H. FISCHER and R. FREY, 1971, Absolute Schweremessungen mit Reversionspendeln in Potsdam 1968-1969. *Veroff. Zentral-instituts Phys. Erde*, **10**, 193.
41) SENDA, O., T. KITSUNEZAKI, T. INOUYE and K. ANDO, 1971, A determination of the acceleration of gravity of the NRLM. *Report of the National Research Laboratory of Metrology*, **20**, 81-173. (in Japanese).
42) STOKES, G G., 1901, On the effect of the internal friction of fluids on the motion of pendulums. *Mathematical and physical papers*, **3**, 1-141.
43) SUZUKI, H., 1976, The International gravity standardization net 1971 and the Japan gravity standardization net 1975. *J. Geod. Soc. Japan*, **22**, 112-129. (in Japanese).
44) TAJIMA, H., 1975, Gravity change associated with earthquakes and land-deformations. *Bull. Earthq. Res. Inst., Univ. Tokyo*, **50**, 209-272. (in Japanese).
45) TATE, D. R., 1966, Absolute value of g at the National Bureau of Standards. *J. Res. Nat. Bur. Stand., Washington.* **70C**, 149.
46) TATE, D. R., 1968, Acceleration due to gravity at the National Bureau of Standards. *J. Res. Nat. Bur. Stand., Washington.* **72C**, 1-20.
47) THULIN, A., 1960, Une détermination absolue de g au pavillon de Breteuil, par la méthode de la chute d'une règle divisée. *Ann. Géophys.* **16**, 105-127.
48) TSUBOKAWA, I., 1970, Summary of general discussion at the Second symposium on gravity survey and precise levelling. *J. Geod. Soc. Japan*, **16**, 76-88. (in Japanese).
49) VOLET, Ch., 1946, Sur la mesure absolue de la gravité. *Comptes Rendus Acad. Sci. Paris*, **222**, 373-375.
50) WALLARD, A. J., J. M. CHARTIER and J. HAMON, 1975, Wavelength measurements of the iodine stabilized helium-neon laser. *Metrologia*, **11**, 89-95.
51) YAMAGISHI, N., 1975, An investigation of microtremors at Matsushiro. *Quart. J. Seismology*, **40**, 33-42. (in Japanese).

---

2. 可搬型重力絶対測定装置

地震研究所 村 田 一 郎

1. 近年，地殻変動や地震等の地球物理現象との関連で，重力の永年変化を検出しようとする試みがなされ始めている．しかしながら，従来の重力測定は，すべて比較測定方式で実施されている．この

ことは，重力の絶対測定が極めて高度の技術を要する作業であることを考えれば当然であり，比較測定方式は測定の軽便性・迅速性という，それなりの利点と意義を有している．しかし，重力計による比較測定には，

1. 仮不動点を必要とし，厳密な意味での変化量の測定は不可能である．
2. 上記のこととも関連するが，比較的狭い地域に，短期間に発生する変化でないと，検出が困難である．
3. 測定器の運搬による，測定精度の低下を避けられない．

といった欠点がある．以上のような比較測定の限界を超えるためには，絶対測定の実施が不可欠であるという観点から，可搬型重力絶対測定装置の開発を進め，今回，一応の実用段階に達したことが確認された．

2. 測定原理は自由落下法であり，落体の落下時間，落下距離の間に成立する，よく知られた関係 ($S=(1/2)gt^2+v_0t+s_0$) を利用するものである．自由落下法は，さらに，投げ上げ法と狭義の自由落下法とに分けられるが，この研究では，装置の簡素化が可能な狭義の自由落下方式を採用した．装置は本体部と記録部とに分けられる．

本体部は，自由落下の行なわれる真空槽と落下距離を測定するための光学系とからなる．寸法は高さ 100 cm，巾 80 cm，奥行 40 cm の程度で，従来の絶対測定装置が施設的に巨大であったのに比べ，格段に小型化されている．

この装置では，0.01 mGal の測定精度を確保することを目標とした．落体の落下距離は 30 cm に設定し，これを He-Ne レーザーの 633 nm の光を利用した光波干渉測長により測定する方式を採用したので，所期測定精度を確保するためには，干渉縞の 1/100 位相までの弁別を要する．落下時間の測定は，Rb 周波数標準に準拠して行なわれ，また，測定電子回路も十分に余裕のある周波数特性をもっているので，時間測定については，0.01 mGal を上まわる影響はないとして差し支えない．

落体として使用される干渉計の反射鏡としては，しばしば，キュービックコーナーが使用されるが，ここでは小型化の可能なキャッツアイを採用した．そのために，落体は質量が僅か 24 g 弱と極めて軽量化された．本体部には，その他，光源レーザー，受光器，排気装置，真空中で落体をとり扱うための内部機構等が付属する．

記録部は，干渉縞を表示するオッシロスコープ，同画面撮影用カメラ，Rb 周波数標準，制御電子回路等からなる．

落体の落下に伴い発生するレーザー光の干渉縞の推移を一定時間間隔でオッシロスコープ画面に表示させ，これを撮影する．この際，オッシロスコープの掃引を Rb 周波数標準からの時間信号で制御することにより，干渉縞（落下距離）と落下時間の関係がつけられる．

干渉測長では，干渉縞数を計数する必要があるが，この装置では，落下距離が時間の 2 次関数であることを利用した独特の方式を開発，採用している．この方式によれば，計数回路は不要となり，測定電子回路は極めて簡単になる．

この記録方式のさらに大きな利点は，別の面にあり，それは，落下中の落体と装置自体との位置関係が逐一記録されるという点である．外来振動や装置の動揺等がそのまま記録されるので，データ処理により，これらの擾乱の影響を除去することが可能となる．絶対測定では，外来振動は最も大きな誤差原因の一つと考えられているので，その影響を除去できるということは，測定精度向上のために極めて好都合ということができる．

3. 一般に，測定値には種々の原因による誤差が含まれる．この装置では，次の各誤差因により測定値に系統・偶然誤差が混入する可能性が予想されたので，各々について，若干の考察と実験を行なった．

1. 光波長の不確定性　2. 時間信号の不確定性　3. 光速度の有限性　4. 重力の鉛直勾配
5. 残存気体の抵抗　6. 光束の非鉛直性　7. 落体の光学特性　8. 電磁気力
9. 信号の遅延　10. 器械振動

その結果，重力測定値に比較的大きな影響を与える誤差因と，その程度は，

光波長の不確定性　20 μGal,
残存気体の抵抗　8 μGal,
重力の鉛直勾配　8 μGal,
器械振動　30 μGal,

であることが明かになった．その他の誤差因の影響は，数 μGal 以下であるか，或いは，大きくても，厳密な修正が可能である．

4. 開発した装置の実際的な性能を確認する目的を含めて，1976年7月，装置を測定現地に運搬して行なう，実用観測を長野県松代気象庁地震観測所で実施した．

現在までに結果の得られた21回の落下についてみると，測定重力値の分散は非常に小さい．また，いずれの落下についても，落下距離の増加の様子は，結果に 3 μGal の誤差を与えるふらつきを示す程度で，順調な落下状態を示している．

得られた結果を測定時刻にしたがって，潮汐曲線に重ねてみると，夫々の落下が，その時点での地球潮汐に応じている様子がうかがわれる．最終結果にまとめる際には，G 値を 1.20 として，潮汐補正を加えた．

実際の落下は有限の真空度の中で行なわれるので，残存気体の影響を受ける．この分の補正のために，実験的に気圧係数を求めた．結果は -2.18×10^3 mGal/Torr であった．一方，理論計算でこの係数は，-1.40×10^3 mGal/Torr となることが予想されていた．実験，理論それぞれに加わる不確定要素を考慮すれば，両数値は良好な一致を示しているとしてよい．全落下の結果を一括して，最小二乗法により完全真空における値を求め，重力値として．

$$g=979\ 769.892\pm0.036\ \text{mGal}$$

を得た．結果につけた誤差は，単観測に対する標準誤差である．

気圧 0 Torr における値	979 769.892 mGal
器械高補正	0.235
光速度補正	0.004
結　果	979 770.131±0.010 mGal

上記のように，必要な補正を加えて，最終結果を得た．誤差は測定結果について得られた ±0.036 mGal に，最終結果を求めるために考慮すべき各種偶然誤差を重ね合せて得られた，平均値に対する標準誤差である．

この装置では，落下距離の増加状況が逐一記録されていることを利用して，測定結果の良否について，ある程度の判断が可能なはずである．事実，落下距離の増加状況の異常な落下から得られた測定値は，平均値に比べ，過大（或いは過小）であることが多く，落下距離の連続記録が結果の良否の判定に有効であることが判明した．これにより，この装置のもつ利点の一つが確認された．

5. 松代の地震観測所には国土地理院の1等重力点が設置されているので，今回の絶対測定の結果と従来の重力測定による重力値と比較することが可能である．

同点における重力値は，日本重力基準網 1975 (JGSN 75) 中の一点として，

$$g_{FGS}=979\ 769.76\pm0.01\ \text{mGal}$$

と与えられている．JGSN 75 に準拠した絶対測定点の重力値は，重力計による結合測定により，

$$g_{ABS}=979\ 770.19\pm0.01\ \text{mGal}$$

であることが判った．この値と今回の絶対測定の結果とのくい違いは 0.06mGal である．しかも，JGSN 75 の絶対値としての誤差は 0.1 mGal 程度はあり得ること．また，絶対測定に使用した，干渉測長用光源レーザーの波長検定を実施することができず，波長は 632.99142 nm であるとした仮定値であること．レーザーの波長は機種間で極端な場合，1×10^{-7} と 0.1 mGal の差異を与える程に異なることがあり得るということを考慮すれば，両者のくい違いは，合理的な範囲に収まっているとみなして差し支えない．

また，両者の測定誤差も ±0.01 mGal と全く同程度であることも判明した．

以上のことから，今回の装置の完成によって，

A. JGSN 75 の採用値には，その誤差を上まわる系統誤差は含まれていないとみて差し支えないこと．

B. 絶対測定が可搬型の装置によっても，比較測定と同程度の測定精度をもって実施できること．

が明かとなった．

この装置の開発により，重力測定の分野に新たな測定手段が加わることになる．そして，このことは，重力永年変化検出の可能性を現実化したことを意味し，この分野に新たな展望をひらくものということができるであろう．

Appendix I
An Example of Interference Fringe

Drop Number 84

Trace number	Amplitude	Frequency	Initial phase	Residual
51	31.60	0.00590	4.090	135.35
52	34.56	0.00603	5.404	66.10
53	28.50	0.00657	5.376	81.48
54	28.21	0.00645	7.152	119.16
55	32.97	0.00658	7.913	51.42
56	29.36	0.00662	8.608	74.98
57	32.47	0.00680	8.372	58.90
58	29.68	0.00700	7.533	62.36
59	26.99	0.00718	6.746	43.75
60	26.86	0.00735	6.010	46.19
61	27.93	0.00740	5.401	35.44
62	27.92	0.00749	4.442	147.84
63	28.81	0.00749	3.495	111.94
64	29.72	0.00769	7.787	97.80
65	28.95	0.00796	5.150	132.86
66	31.84	0.00814	9.097	110.02
67	29.00	0.00788	7.668	69.84
68	30.74	0.00811	4.480	105.39
69	30.93	0.00836	7.150	119.87
70	31.16	0.00857	3.430	184.94
71	28.56	0.00867	6.266	80.24
72	31.11	0.00863	8.996	54.28
73	28.40	0.00906	3.706	53.76
74	28.42	0.00907	5.574	31.78
75	29.63	0.00908	7.671	56.19
76	28.16	0.00946	7.867	116.50
77	28.60	0.00960	8.844	148.24
78	25.78	0.00934	5.005	149.53
79	30.07	0.00943	5.493	264.84
80	30.27	0.00981	5.040	70.19
81	31.06	0.00993	4.897	103.07
82	27.75	0.00994	5.054	167.52
83	34.93	0.01005	4.356	88.14
84	30.92	0.01013	3.704	105.82
85	30.23	0.01021	8.818	116.69
86	33.73	0.01029	7.614	142.75
87	29.63	0.01052	5.442	174.93
88	32.69	0.01058	7.099	68.62

(to be continued)

(continued)

Trace number	Amplitude	Frequency	Initial phase	Residual
89	29.81	0.01074	4.657	143.92
90	29.12	0.01069	8.962	137.05
91	30.66	0.01111	5.173	122.68
92	28.89	0.01134	7.842	88.31
93	29.16	0.01106	6.024	307.17
94	27.79	0.01141	7.898	97.55
95	30.25	0.01144	4.545	120.78
96	28.15	0.01181	5.783	105.83
97	30.94	0.01182	8.364	128.55
98	27.35	0.01190	3.752	145.51
99	28.21	0.01203	5.019	80.57
100	26.72	0.01216	5.918	57.96
101	29.81	0.01217	6.916	69.45
102	30.26	0.01223	7.656	242.96
103	30.37	0.01248	7.416	146.46
104	31.02	0.01245	8.030	353.91
105	28.21	0.01274	7.219	115.76
106	29.61	0.01301	6.227	111.49
107	28.24	0.01288	6.030	114.74
108	28.15	0.01324	4.450	142.13
109	26.97	0.01316	3.560	75.33
110	27.85	0.01343	7.902	82.77
111	27.66	0.01343	6.645	189.78
112	31.87	0.01383	3.375	158.62
113	27.62	0.01354	8.930	129.72
114	28.31	0.01356	6.437	43.30
115	25.29	0.01387	9.404	128.76
116	26.86	0.01416	5.197	160.79
117	28.99	0.01416	8.497	248.71
118	31.02	0.01432	4.306	165.06
119	30.74	0.01460	5.919	163.91
120	29.89	0.01454	5.908	138.30
121	31.47	0.01467	7.365	151.97
122	28.13	0.01473	9.090	77.02
123	33.03	0.01520	8.794	112.60
124	29.90	0.01518	4.112	87.35
125	26.71	0.01507	5.129	93.07
126	30.00	0.01540	4.914	114.60
127	28.72	0.01561	4.390	70.46
128	30.61	0.01575	4.265	111.27
129	27.84	0.01579	4.016	203.80

(to be continued)

(continued)

Trace number	Amplitude	Frequency	Initial phase	Residual
130	27.63	0.01585	3.552	78.01
131	28.50	0.01599	8.690	87.96
132	28.98	0.01611	7.050	209.52
133	25.94	0.01599	6.445	130.50
134	33.89	0.01638	3.365	114.98
135	31.25	0.01649	7.612	103.68
136	28.08	0.01652	5.422	104.06
137	28.60	0.01660	9.412	140.21
138	28.21	0.01680	6.284	111.68
139	30.35	0.01709	8.710	159.07
140	28.91	0.01718	5.323	60.55
141	28.43	0.01726	7.964	164.36
142	27.07	0.01736	3.932	82.99
143	29.75	0.01740	6.232	93.89
144	29.88	0.01755	7.993	60.18
145	28.38	0.01769	9.307	91.83
146	26.85	0.01779	4.407	184.83
147	25.71	0.01786	5.315	117.88
148	30.17	0.01790	6.262	183.96
149	28.68	0.01814	5.952	204.25
150	30.09	0.01835	5.626	321.65
151	27.08	0.01838	5.751	173.43
152	27.13	0.01874	4.310	151.62
153	29.81	0.01865	8.797	70.96
154	26.91	0.01891	7.122	53.15
155	31.03	0.01898	6.273	112.77
156	28.86	0.01879	5.510	84.22
157	28.56	0.01929	8.684	102.47
158	25.46	0.01918	7.250	127.71
159	29.57	0.01954	3.926	75.80
160	25.75	0.01934	8.753	41.03
161	26.17	0.01967	5.061	237.33
162	25.76	0.01976	8.375	92.90
163	28.07	0.02009	4.063	106.09
164	25.47	0.01994	7.730	104.81
165	25.44	0.02018	9.352	91.27
166	27.00	0.02020	5.494	114.53
167	27.45	0.02046	6.407	120.12
168	28.56	0.02036	8.922	70.21
169	25.85	0.02045	4.023	122.01
170	30.72	0.02076	4.258	88.03

(to be continued)

(continued)

Trace number	Amplitude	Frequency	Initial phase	Residual
171	26.13	0.02093	4.885	87.43
172	26.67	0.02102	5.236	78.38
173	25.48	0.02105	5.836	150.24
174	24.58	0.02120	5.214	158.50
175	29.70	0.02139	4.672	98.35
176	25.20	0.02165	3.194	248.22
177	28.05	0.02152	3.236	205.45
178	25.33	0.02173	7.971	168.04
179	28.71	0.02199	5.984	115.33
180	28.38	0.02201	4.555	232.55
181	28.09	0.02198	9.293	55.73
182	23.71	0.02219	6.688	182.00
183	26.64	0.02242	3.327	119.58
184	27.69	0.02250	7.344	62.60
185	29.25	0.02241	4.846	127.78
186	29.43	0.02281	6.962	51.83
187	25.71	0.02288	3.358	78.96
188	29.31	0.02305	5.644	170.64
189	26.11	0.02318	7.644	158.86
190	27.05	0.02309	3.833	113.04
191	24.32	0.02302	6.084	90.27
192	28.61	0.02359	5.460	177.70
193	23.66	0.02380	6.242	108.38
194	25.82	0.02362	7.900	191.58
195	26.02	0.02400	7.668	157.99
196	25.24	0.02391	8.448	156.11
197	25.27	0.02405	8.552	135.95
198	25.69	0.02423	7.647	126.37
199	26.99	0.02452	6.262	178.90
200	26.79	0.02446	5.996	117.46
201	27.88	0.02451	4.916	86.58
202	24.43	0.02489	8.768	120.13
203	26.90	0.02486	7.725	76.19
204	28.42	0.02507	5.426	160.42
205	23.45	0.02500	3.670	135.67
206	27.45	0.02532	6.862	122.21
207	26.11	0.02534	4.160	307.61
208	27.46	0.02544	7.399	216.64
209	24.16	0.02565	3.560	244.21
210	28.40	0.02547	7.306	82.33
211	25.04	0.02562	3.357	230.13

(to be continued)

(continued)

Trace number	Amplitude	Frequency	Initial phase	Residual
212	24.64	0.02579	5.122	76.56
213	21.43	0.02603	6.892	112.76
214	23.16	0.02600	8.777	212.29
215	22.21	0.02612	3.993	185.83
216	25.16	0.02652	7.874	143.23
217	26.57	0.02633	3.551	98.24
218	24.57	0.02665	9.372	120.28
219	25.87	0.02695	9.173	110.90
220	22.01	0.02712	9.028	85.47
221	23.76	0.02691	3.694	142.80
222	23.35	0.02699	3.276	144.20
223	24.05	0.02726	7.950	75.79
224	25.68	0.02740	6.810	88.70
225	22.32	0.02745	5.324	129.37
226	24.24	0.02733	4.640	152.56
227	20.96	0.02785	7.314	230.61
228	23.45	0.02762	6.610	25.83
229	21.33	0.02809	9.277	96.04
230	21.18	0.02834	5.919	132.47
231	20.66	0.02795	4.936	129.34
232	23.55	0.02863	5.522	142.49
233	22.74	0.02827	3.737	194.60
234	25.44	0.02904	3.406	125.69
235	24.49	0.02870	7.684	307.93
236	24.64	0.02880	9.367	270.93
237	27.30	0.02877	5.693	153.39
238	26.40	0.02905	6.261	118.60
239	30.05	0.02899	8.144	67.82
240	23.46	0.02923	8.343	239.82
241	24.96	0.02951	8.224	155.97
242	24.76	0.02944	8.933	144.64
243	24.44	0.03010	6.925	306.17
244	24.24	0.02986	8.139	82.36
245	21.24	0.02999	7.315	115.15
246	24.01	0.02982	8.021	99.08
247	22.97	0.03037	8.616	140.64
248	22.54	0.03046	7.481	280.96
249	21.83	0.03050	5.801	129.15
250	26.85	0.03077	3.266	176.08
251	23.06	0.03078	7.741	214.88
252	24.59	0.03074	6.213	109.83

(to be continued)

(continued)

Trace number	Amplitude	Frequency	Initial phase	Residual
253	25.35	0.03101	3.150	114.87
254	25.28	0.03118	6.235	92.08
255	25.66	0.03115	4.112	202.72
256	23.57	0.03155	5.820	118.77

Note: Amplitude, frequency and residual are represented on a arbitrary linear scale. Initial phases are distributed in the range between π and 3π.

Appendix II
An Example of Synthesized Fringe Count

Drop Number 84

Sampling number	Fringe count	Second difference	Deviation
51	0.09		0.0121
52	15.37	31.03	−0.0164
53	61.68	30.91	0.0250
54	138.90	30.98	0.0155
55	247.09	30.94	0.0291
56	386.23	30.93	0.0238
57	556.29	30.97	−0.0033
58	757.33	30.94	−0.0199
59	989.31	31.01	−0.0513
60	1252.29	30.94	−0.0287
61	1546.22	30.98	−0.0233
62	1871.13	30.94	0.0024
63	2226.97	30.96	0.0116
64	2613.78	30.93	0.0237
65	3031.51	31.00	0.0123
66	3480.25	30.88	0.0420
67	3959.87	31.01	−0.0016
68	4470.50	30.94	0.0052
69	5012.07	30.97	−0.0014
70	5584.60	30.97	0.0014
71	6188.11	30.91	0.0170
72	6822.52	31.00	−0.0190
73	7487.93	30.90	−0.0125
74	8184.24	31.03	−0.0649
75	8911.57	30.92	−0.0479
76	9669.83	30.98	−0.0652

(to be continued)

(continued)

Sampling number	Fringe count	Second difference	Deviation
77	10459.07	31.00	−0.0603
78	11279.30	30.90	−0.0129
79	12130.44	31.02	−0.0224
80	13012.59	30.89	0.0276
81	13925.63	30.99	0.0136
82	14869.67	30.92	0.0313
83	15844.62	30.99	0.0136
84	16850.57	30.91	0.0289
85	17887.42	31.00	0.0004
86	18955.28	30.93	0.0144
87	20054.07	31.00	0.0024
88	21183.85	30.91	0.0331
89	22344.55	30.96	0.0166
90	23536.21	30.96	0.0064
91	24758.83	30.93	0.0029
92	26012.39	31.00	−0.0291
93	27296.94	30.93	−0.0132
94	28612.43	31.00	−0.0234
95	29958.92	30.91	0.0090
96	31336.31	31.02	−0.0066
97	32744.73	30.90	0.0410
98	34184.04	30.96	0.0279
99	35654.31	30.95	0.0154
100	37155.52	30.95	−0.0086
101	38687.69	30.99	−0.0388
102	40250.84	30.94	−0.0397
103	41844.93	30.99	−0.0526
104	43470.02	30.94	−0.0338
105	45126.04	30.97	−0.0323
106	46813.03	30.91	−0.0213
107	48530.93	31.04	−0.0570
108	50279.87	30.87	−0.0079
109	52059.69	31.02	−0.0429
110	53870.52	30.97	−0.0139
111	55712.32	30.90	0.0248
112	57585.02	31.03	0.0021
113	59488.75	30.88	0.0533
114	61423.36	31.02	0.0320
115	63389.00	30.85	0.0784
116	65385.49	31.03	0.0229
117	67413.01	30.90	0.0392

(to be continued)

(continued)

Sampling number	Fringe count	Second difference	Deviation
118	69471.43	30.99	0.0013
119	71560.84	31.00	−0.0078
120	73681.25	30.90	0.0225
121	75832.55	31.01	−0.0024
122	78014.87	30.91	0.0215
123	80228.09	31.03	−0.0044
124	82472.33	30.86	0.0387
125	84747.43	31.05	−0.0192
126	87053.58	30.89	0.0147
127	89390.62	31.02	−0.0160
128	91758.68	30.92	0.0149
129	94157.66	30.98	0.0112
130	96587.62	30.94	0.0268
131	99048.52	30.90	0.0277
132	101540.33	31.03	−0.0245
133	104063.16	30.90	−0.0025
134	106616.90	31.01	−0.0398
135	109201.63	30.94	−0.0281
136	111817.31	31.00	−0.0376
137	114463.99	30.94	−0.0014
138	117141.60	30.94	0.0154
139	119850.15	30.96	0.0143
140	122589.67	30.95	0.0188
141	125360.13	30.95	0.0157
142	128161.55	30.97	0.0069
143	130993.94	30.98	0.0146
144	133857.30	30.92	0.0428
145	136751.59	30.99	0.0334
146	139676.87	30.90	0.0604
147	142633.05	30.99	0.0340
148	145620.23	30.91	0.0450
149	148638.32	30.98	0.0112
150	151687.38	30.97	0.0004
151	154767.42	30.94	0.0009
152	157878.40	31.02	−0.0156
153	161020.39	30.89	0.0293
154	164193.27	31.03	0.0043
155	167397.18	30.85	0.0519
156	170631.95	31.04	−0.0027
157	173897.75	30.91	0.0212
158	177194.46	30.98	−0.0062

(to be continued)

(continued)

Sampling number	Fringe count	Second difference	Deviation
159	180522.14	30.96	−0.0128
160	183880.79	30.96	−0.0144
161	187270.39	30.98	−0.0124
162	190690.98	30.92	0.0111
163	194142.48	30.99	−0.0010
164	197624.98	30.90	0.0213
165	201138.38	31.00	−0.0125
166	204682.78	30.89	0.0001
167	208258.07	31.05	−0.0508
168	211864.41	30.93	−0.0114
169	215501.69	30.95	0.0028
170	219169.91	30.98	0.0079
171	222869.11	30.91	0.0348
172	226599.22	31.00	0.0142
173	230360.33	30.88	0.0414
174	234152.32	31.03	−0.0093
175	237975.35	30.89	0.0170
176	241829.27	31.01	−0.0218
177	245714.20	30.94	−0.0055
178	249630.07	30.97	−0.0014
179	253576.91	30.94	0.0131
180	257554.69	30.96	0.0107
181	261563.43	30.97	0.0091
182	265603.14	30.89	0.0210
183	269673.74	31.02	−0.0369
184	273775.35	30.93	−0.0312
185	277907.91	31.02	−0.0477
186	282071.48	30.89	0.0001
187	286265.94	31.00	−0.0160
188	290491.41	30.93	0.0088
189	294747.80	30.95	0.0070
190	299035.14	30.97	−0.0030
191	303353.46	30.92	0.0025
192	307702.69	31.01	−0.0286
193	312082.94	30.91	−0.0022
194	316494.10	31.03	−0.0229
195	320936.29	30.88	0.0294
196	325409.36	31.03	0.0076
197	329913.45	30.87	0.0539
198	334448.42	30.98	0.0127
199	339014.36	30.98	−0.0063

(to be continued)

(continued)

Sampling number	Fringe count	Second difference	Deviation
200	343611.29	30.93	0.0010
201	348239.15	30.97	−0.0191
202	352897.98	30.99	−0.0222
203	357587.80	30.94	0.0050
204	362308.55	30.92	0.0133
205	367060.23	31.02	−0.0107
206	371842.93	30.88	0.0263
207	376656.51	30.99	−0.0119
208	381501.08	30.94	−0.0139
209	386376.60	30.98	−0.0316
210	391283.09	30.97	−0.0273
211	396220.55	30.92	−0.0144
212	401188.93	31.05	−0.0378
213	406188.35	30.85	0.0281
214	411218.63	31.03	−0.0088
215	416279.94	30.85	0.0300
216	421372.10	31.04	−0.0407
217	426495.30	30.90	−0.0241
218	431649.41	31.03	−0.0613
219	436834.55	30.94	−0.0253
220	442050.62	30.96	−0.0092
221	447297.65	30.95	0.0093
222	452575.63	30.91	0.0208
223	457884.53	31.00	−0.0124
224	463224.42	30.90	0.0001
225	468595.22	31.03	−0.0473
226	473997.04	30.90	−0.0233
227	479429.76	31.03	−0.0574
228	484893.51	30.93	−0.0133
229	490388.20	30.92	0.0049
230	495913.81	31.02	−0.0128
231	501470.43	30.85	0.0326
232	507057.91	31.04	−0.0313
233	512676.42	30.86	−0.0138
234	518325.80	31.12	−0.0897
235	524006.29	30.83	−0.0055
236	529717.61	31.08	−0.0496
237	535460.01	30.85	0.0267
238	541233.26	31.02	−0.0053
239	547037.53	30.89	0.0266
240	552872.69	30.98	−0.0033

(to be continued)

(continued)

Sampling number	Fringe count	Second difference	Deviation
241	558738.83	30.93	−0.0139
242	564635.90	30.98	−0.0485
243	570563.95	31.01	−0.0610
244	576523.01	30.88	−0.0188
245	582512.96	31.08	−0.0550
246	588533.97	30.84	0.0275
247	594585.82	31.02	−0.0111
248	600668.69	30.89	0.0116
249	606782.45	31.01	−0.0363
250	612927.21	30.96	−0.0359
251	619102.93	31.02	−0.0369
252	625309.67	30.94	0.0237
253	631547.34	30.92	0.0671
254	637815.93	31.05	0.0719
255	644115.58	30.87	0.1707
256	650446.10		0.1869